Ricardo Manuel Garcia Estevinho

Degree in Biotechnology

Insight into Catalytic Features of Native and Engineered Laccases and Synthesis of Added-Value Compounds

Dissertation for the degree of Master in Biotechnology

Supervisor: Prof.ª Dr.ª Lígia Oliveira Martins, Principal Investigator, Instituto de Tecnologia Química e Biológica António Xavier/Universidade Nova de Lisboa

Co-supervisor: Dr.ª Vânia Brissos, Assistant Researcher, Instituto de Tecnologia Química e Biológica António Xavier/Universidade Nova de Lisboa

December, 2020

Ricardo Manuel Garcia Estevinho

Degree in Biotechnology

Insight into Catalytic Features of Native and Engineered Laccases and Synthesis of Added-Value Compounds

Dissertation for the degree of Master in Biotechnology

Supervisor: Prof.ª Dr.ª Lígia Oliveira Martins, Principal Investigator, Instituto de Tecnologia Química e Biológica António Xavier/Universidade Nova de Lisboa

Co-supervisor: Dr.ª Vânia Brissos, Assistant Researcher, Instituto de Tecnologia Química e Biológica António Xavier/Universidade Nova de Lisboa

December, 2020

Insight into Catalytic Features of Native and Engineered Laccases and Synthesis of Added-Value Compounds

Agradecimentos

A elaboração deste trabalho final de mestrado não teria sido possível sem esforço, compromisso, resiliência e o auxílio direto e indireto de diversas pessoas, às quais dedico este trabalho e, nesta secção, declaro os meus agradecimentos.

Em primeiro lugar, agradecer à Dr.ª Lígia Oliveira Martins por me ter permitido realizar o último ano de mestrado no seu laboratório, Microbial Enzyme Technology (MET), onde vivi novas experiências que me fizeram crescer como pessoa e como profissional de ciência. O apoio, disponibilidade e orientação por ela proporcionados, juntamente com a sua contagiante paixão pela ciência, foram uma grande influência para mim e vitais para o desenvolvimento do meu trabalho.

À Dr.ª Vânia Brissos por me encaminhar na direção certa e se importar de forma consistente com a qualidade do meu trabalho e com a minha evolução enquanto profissional de ciência. Percebeu com relativa facilidade as minhas qualidades e falhas e foi por isso que conseguiu, de muitas maneiras, retirar o melhor de mim para que eu pudesse realizar este trabalho.

À Dr.ª Paula Robalo por me ter aberto as portas ao seu laboratório no Instituto Superior de Engenharia de Lisboa para a última fase do meu trabalho de mestrado. A sua intenção em adicionar conteúdo de qualidade ao meu trabalho foi determinante para a realização do mesmo. O seu laboratório tem uma parceria muito interessante com o MET e, ao ter trabalhado em ambos, fez que a minha experiência de tese de mestrado fosse bastante completa.

A todo o staff do MET, a Helena, o Diogo, o André, o Mário, a Margarida, a Magali, a Magdalena e Carolina, e ao staff do laboratório da Dr.ª Paula Robalo, por me ajudarem em tudo o que precisei.

Aos meus pais, irmã, avó e tio por terem feito tudo ao seu alcance para tornar todo este trabalho possível. O seu apoio incondicional e a sua constante crença nos meus feitos foram um grande suporte.

À Patrícia, que foi fundamental para ultrapassar todos os obstáculos que tive de enfrentar durante este período e me encaminhar sempre no rumo certo.

Aos meus amigos, da minha cidade natal e aos que fiz durante o meu período académico, por torcerem pelo meu sucesso e manifestarem interesse no meu trabalho, perguntando-me, de tempos em tempos, em que fase de desenvolvimento estava e se estava a ir de acordo com os objetivos propostos.

Este ano vivenciámos uma pandemia à escala global, dificultando a qualidade de vida, bem como a acessibilidade e condições de trabalho. No entanto, nem isso tirou força a todos estes intervenientes para continuar o desenvolvimento do meu e dos seus projetos, o que me fez sentir profundamente feliz e sortudo por estar acompanhado por este incrível conjunto de pessoas. Por isso, a todos, o meu muito obrigado!

Resumo

As *multicopper oxidases* são uma família de enzimas que catalisa a oxidação de substratos acoplada à redução do O_2 em água. Esta família divide-se em metalo-oxidases, que oxidam preferencialmente iões metálicos de baixa valência e lacases, que oxidam mais eficazmente compostos orgânicos. As lacases têm uma capacidade redox notável nos processos de degradação e conversão da lenhina.

Neste estudo, avaliou-se a eficiência catalítica (k_{cat}/K_m) das variantes 15E6-loop5 e 23B3 para compostos fenólicos derivados da lenhina. Estas variantes foram obtidas através de evolução laboratorial da metalo-oxidase McoA de *Aquifex aeolicus*. As enzimas foram produzidas, purificadas e caracterizadas bioquimicamente. Compararam-se os parâmetros cinéticos para os fenólicos (do tipo siringil, guaiacil e p-hidroxifenil) com os da enzima modelo CotA-lacase. A CotA-lacase oxidou todos os treze substratos, enquanto as variantes da McoA oxidaram oito. Para estes, as variantes da McoA mostraram valores de k_{cat}/K_m semelhantes aos da CotA. Os melhores substratos foram álcool sinapílico > álcool coniferílico > ácido cafeico, mostrando a importância dos substituintes *orto* e *para* nas velocidades de oxidação. Em geral, a variante 15E6-loop5 é um melhor biocatalista do que 23B3.

Testou-se a bioconversão do álcool sinapílico, álcool coniferílico e ácido cafeico em siringaresinol, pinoresinol e fenilinsina A, respectivamente, compostos com interessantes propriedades farmacêuticas. O resultado mais promissor obteve-se com álcool sinapílico a pH 10, resultando num maior rendimento de conversão de siringaresinol, conforme avaliado por RMN de protões, com a CotA do que com a 15E6-loop5. A pH 8, ótimo para a atividade enzimática, não foi detetado siringaresinol, indicando a importância da desprotonação do álcool sinapílico (pKa = 9,4) na reação alvo. Além das suas propriedades medicinais, o siringaresinol, com dois fenóis e uma porção bis-furânica cis-fundida rígida, é um importante substituto do bisfenol A, um composto oriundo do petróleo usado como monómero em plásticos de policarbonato e resinas epóxi.

Palavras-Chave

Valorização da lenhina; Fenólicos; Álcool sinapílico; Siringaresinol; Lacases

Abstract

Multicopper oxidases are a family of enzymes that catalyze the oxidation of substrates coupled to the reduction of molecular oxygen to water. This family can be divided in metallo-oxidases that preferably oxidize low-valence metal ions and, laccases that oxidize organic compounds more efficiently. Laccases have a remarkable redox capability in lignin degradation and conversion processes.

In the present study, the catalytic efficiency (k_{cat}/K_m) of engineered 15E6-loop5 and 23B3 variants, obtained through laboratory evolution of the *Aquifex aeolicus* metallo-oxidase McoA, was evaluated towards a set of lignin-related phenolics. The enzymes were produced, purified and biochemically characterized. The kinetic parameters for the tested phenolics (syringyl, guaiacyl and *p*-hydroxyphenyl type) were compared with those of model enzyme CotA-laccase. CotA-laccase was able to oxidize all thirteen substrates while McoA-variants only oxidized eight. However, for these, the McoA variants showed similar k_{cat}/K_m values to CotA. The best substrates were sinapyl alcohol > coniferyl alcohol > caffeic acid, showing the importance of *ortho* and *para* substituents in the oxidation rates. Overall, 15E6-loop5 exhibited slightly improved performance than 23B3 variant.

Bioconversion of sinapyl alcohol, coniferyl alcohol and caffeic acid into syringaresinol, pinoresinol and phenillinsin A, respectively, known to exhibit interesting medical properties, were carried out. The most promising result was obtained with sinapyl alcohol and this reaction was further optimized, resulting in a higher yield of conversion to syringaresinol, as assessed by ^{1}H NMR, with CotA than 15E6-loop. At pH 8, the optimal pH for enzymes´ activity no syringaresinol was observed, pointing out to the importance of sinapyl alcohol deprotonation (pKa = 9.4) in the target reaction. Beside its potential medical uses, syringaresinol, with its two phenols and its rigid cis-fused bis-furanic moiety, is an important substitute of bisphenol A, a petro based compound used as monomer in polycarbonate plastics and epoxy resins.

Keywords

Lignin valorization; Phenolics; Sinapyl alcohol; Syringaresinol; Laccases

List of Contents

Page:

List of Figures

Page:

List of Tables

Page:

Abbreviations

2,6-DMP – 2,6-Dimethoxyphenol

ABTS - 2,2'-Azino-bis(3-ethylbenzthiazoline-6-sulfonic acid)

BCA - Bicinchoninic acid

BR – Britton-Robinson

BSA – Bovine serum albumine

CE_{80} – Crude extract heated at 80°C

CV – Coefficient of variance

Da – Dalton

DMSO - Dimethyl sulfoxide

DNA - Deoxyribonucleic acid

ε - Molar extinction coefficient

epPCR – Error prone Polymerase Chain Reaction

IPTG - Isopropyl β-D-1-thiogalactopyranoside

LA – Luria-Bertani with agar

LB – Luria-Bertani

LDA – Lignin-degrading auxilary

LME – Lignin modifying enzymes

LMS – Laccase mediator system

MCO – Multicopper oxidase

NHE – Normal hydrogen electrode

^{1}H NMR – Proton nuclear magnetic resonance

OD_{600} – Optical Density at 600 nm

PAL - Phenylalanine lyase

rpm – Rotations per minute

SDS-PAGE - Sodium dodecyl sulfate polyacrylamide gel electrophoresis

SHE - Standard hydrogen electrode

T1Cu – Type 1 copper

T2Cu – Type 2 copper

T3Cu – Type 3 copper

TB – Terrific Broth

TLC – Thin-layer chromatography

TNC – Trinuclear cluster

UV – Ultraviolet

1. Introduction

1.1 Refineries *vs* Biorefineries

The basic function of a refinery is to separate the raw fossil feedstock material into various fractions that will feed a variety of industries and end-user markets. Since the 1860s that the industrial process to refine crude oil into essential products for mankind such as energy, transportation fuels and chemicals is well established (Clews, 2016; Strassberger et al., 2014). However, fossil resources (e.g., oil, coal and natural gas) are limited and its depletion is mostly related with their use under a linear economy concept. As such, these resources no longer accomplish, in a sustainable manner, the supply for needed products, materials, energy and fuels (Dávila et al., 2019). Additionally, since the increased consumption of fossil-based raw feedstocks adversely affects the natural ecosystems (e.g. resulting in greenhouse gas emissions arising from fossil fuel combustion), they constitute serious risks to human health. Therefore, renewable and sustainable alternatives have been developed to meet the increasing fuel demands (Bilal & Iqbal, 2020; Kamm et al., 2006; Shu et al., 2020; Strassberger et al., 2014; Tolbert et al., 2014).

Biomass, which is any organic matter of animal or plant origin composed of hydrogen, oxygen, nitrogen, sulfur and phosphorous atoms, plus small quantities of heavy metals, spontaneous or cultivated by humans, terrestrial or marine, produced directly or indirectly through the process of photosynthesis is considered a renewable resource on a human timescale (Bonechi et al., 2017; Strassberger et al., 2014). Refinery of biomass, or biorefinery, carries out physical, chemical or biological technologies so biomass can be degraded into their building blocks (e.g., sugars, proteins, triglycerides), for later conversion into energy (e.g., biofuels, heat/electricity), materials (e.g., polymers) or chemical products (e.g., aromatic compounds). This can be performed with reduced emission of greenhouse gases, with zero waste generation and leading to a circular economy, by considering dead biomass or biological waste as a valuable feedstock, accomplishing the reduction, the reuse and the recycling of wastes. This concept of biorefinery is not a new one, in fact, breweries and pulp industries fit the definition of a biorefinery regarding their usage of biomass (Kamm & Kamm, 2004; Konwar et al., 2018; Zakzeski et al., 2010).

The feedstocks more commonly collected and stored by industries for production of added-value products are from plant origin due to their higher abundance compared with animal biomass, so biomass in a biorefinery context is often referred to plant based materials. An important characteristic in plant biomass utilization is the carbon neutrality cycle, which is possible since the CO_2 released by certain biorefinery processes (e.g., combustion), is recycled by plants via photosynthesis (Figure 1.1). Moreover, biomass from plant origin has high bio-conversion potential, reduced cost and does not compromise food, feed and fiber (Bonechi et al., 2017; Capolupo & Faraco, 2016; Cherubini, 2010; Ragauskas et al., 2014; Yousuf, 2012). Hence, feedstocks for biorefinery are generally derived from agriculture, forestry, municipal solid wastes and aquaculture (Figure 1.1) (Pande & Bhaskarwar, 2012). Agricultural products, such as food products (e.g. cereal, grasses and green plants) and agricultural residues are considered. These feedstocks, if correctly processed, can lead to high-value useful products in the food, pharmaceutical and cosmetic industries (Bonechi et al., 2017; Pande &

Bhaskarwar, 2012). Forest biomass is mainly divided into two categories, forest residues (e.g. dead trees, forest-fire remains) and waste generated during manufacture of wood products (e.g. residues from pulp and paper manufacture), and can be used without jeopardizing the forest vegetation. Municipal solid wastes (e.g. animal waste, crop residues or industrial waste) can be used for energy or material production leading to a reduction of wastes to municipal landfills, which consequently reduces gas emissions up to the atmosphere (Pande & Bhaskarwar, 2012). Biorefineries based on aquaculture rely on algae which are the most photosynthetically efficient organisms on earth. Like plants, algae use photosynthesis to convert solar energy into chemical energy and store it in the form of high energy substances such as oils, carbohydrates, and proteins. In plants, the predominant storehouse of this chemical energy is carbohydrates but in algae, this energy is stored in the form of oils. The oil is often extracted by solvent extraction and can be used as fuel or can be converted into biodiesel (Pande & Bhaskarwar, 2012).

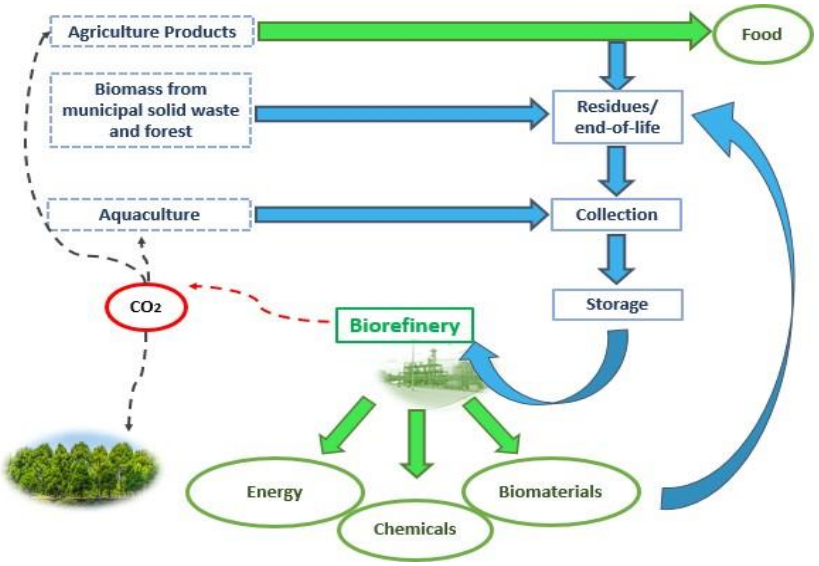

Figure 1.1: A circular economy in the processing of biomass of plant origin. Adapted from Bonechi et al. (2017).

There are several biorefinery categories. The characterization is based on the feedstock utilized, the technology applied or the product obtained. A category that has been considered one of the most relevant in the past few decades is the lignocellulose biorefinery, due to the fact that the feedstock material (i.e., lignocellulosic biomass) is the most abundant organic renewable resource on earth (Konwar et al., 2018; Zheng et al., 2017).

1.2 Chemical characterization of lignocellulosic biomass

Lignocellulosic biomass, which is found in wood, herbaceous crops, forestry and agricultural residues, is a term used for organic vegetable matter, composed of carbohydrates (cellulose and hemicellulose), lignin and minor components such as pectins, glycosylated proteins and ash (McKendry, 2002; Zheng et al., 2017). The lignocellulosic cell wall is divided into two parts, the primary cell wall and the secondary cell wall. The matrix of the primary cell wall is composed of cellulose and hemicellulose,

while in the secondary cell wall, cellulose is deposited with hemicellulose and lignin. These organic components are strongly intermeshed and chemically bonded by non-covalent forces and by covalent cross-linkages (Gupta & Turner, 2017). Cellulose and hemicellulose are composed of polymers of sugars. Lignin, on the other hand, is a non-phenolic polymer that fills the spaces between cellulose and hemicellulose, acting like a resin that holds the lignocellulose matrix together, which contributes to the resistance and protection of the strong cell wall structure. Indeed, these three polymers form a natural and strong biocomposite that aids trees to withstand hostile weather and to support their weight (Ázar et al., 2020; Janusz et al., 2017; Pérez et al., 2002; Zakzeski et al., 2010; Zheng et al., 2017).

1.2.1 Cellulose

Cellulose is the most abundant natural polymer and the largest available organic compound on earth (Zheng et al., 2017). It is the main structural component of lignocellulose cell wall, accounting for 30-50% of the dry weight of lignocellulose (Foyle et al., 2007). It is a linear homopolymer composed of 2,000-26,500 of D-glucose units linked by β-1,4 glycosidic bonds, thus forming cellobiose molecules. A single chain of cellobiose molecules forms an elemental fibril that has hydroxylic groups present in its surface, allowing the connection to other elemental fibrils by van der Waals forces and two to three inter chains of hydrogen bonds (Figure 1.2) (Gupta & Turner, 2017; Higuchi et al., 1997; Pérez et al., 2002; Zheng et al., 2017). The elemental fibrils are arranged in microfibrils with tensile strength, aiding in the stability of plant structures. This suggests that cellulose is a biomaterial with superior mechanical properties, playing an integral role in keeping the structure of plant cell walls stable, exhibiting 60% of water retention (Brigham, 2018; Klemm et al., 2005).

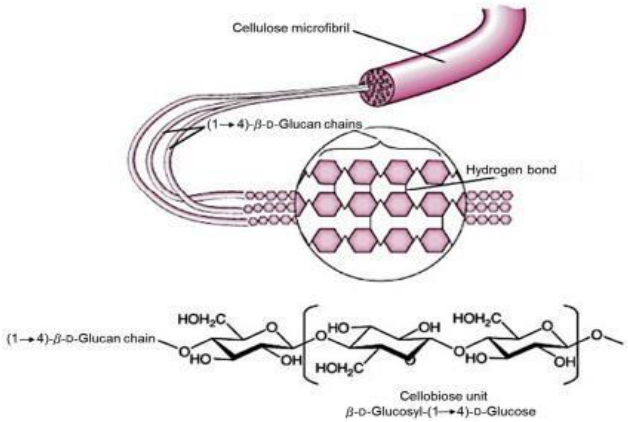

Figure 1.2: Cellulose molecular structure. Adapted from Höfte et al. (2007).

This important polysaccharide can be degraded by the action of microbial cellulases to glucose monomers, which can be subsequently converted to other added-value chemicals (Abdel-Hamid et al., 2013).

1.2.2 Hemicellulose

The second polysaccharide component of lignocellulose is hemicellulose. It is the second most abundant natural polymer carbohydrate on earth and falls in the range of 15-35% of the plant cell wall (Scheller et al., 2010; Zheng et al., 2017). Unlike cellulose, hemicellulose has low molecular weight and a random non-linear structure that varies in polysaccharide content among biomass type. It is heterogeneously composed of polysaccharides like pentoses (xylose and arabinose), hexoses (mannose, glucose, galactose and rhamnose) and acetylated sugars. These sugars are linked by β-1,4- and occasionally β-1,3-glycosidic bonds (Bilal & Iqbal, 2020; Pérez et al., 2002; Zheng et al., 2017). Hemicellulose has lateral chains involved in a network via hydrogen bond with cellulose microfibrils and interacts with lignin via covalent bonds, rendering an extremely rigid matrix of cellulose-hemicellulose-lignin (Zheng et al., 2017).

Due to its amorphous structures and low molecular weight properties, hemicellulose can be easily hydrolyzed by diluted acid or base as well as through the action of microbial hemicellulases. A complex set of enzymes are able to remove the side chains and randomly attack the polymer backbone to release oligosaccharides that are subsequently degraded to simple sugars (Scheller & Ulvskov, 2010).

1.2.3 Lignin

The third main component of lignocellulose is lignin (Latin *lignum* 'wood'). Lignin is the second most abundant organic polymer on earth, and accounts for 15-40% of the lignocellulose cell wall, more specifically, approximately 24-33% in softwoods (e.g., gymnosperm trees), 19–28% in hardwoods (e.g., angiosperm trees) and 15-25% in cereal straws, bamboo or bagasse (Ragauskas et al., 2014; Vassão, et al., 2008; Zheng et al., 2017). Lignin strengthens the plant cell walls by adhesion of layers of cellulose microfibrils, which allows plants to expand significantly in body size and efficiently transport nutrients and water. Moreover, it is also directly related to land plants evolution by enabling them to develop upright forms for an erect growth habit (Janusz et al., 2017).

Lignin is a three-dimensional amorphous, heterogeneous and aromatic biopolymer composed of phenolic (10-20 %) and non-phenolic units (80-90 %) interlinked by a variety of ether and carbon-carbon linkages (Barros et al., 2015; Kawai et al., 1999). These bonds are not susceptible to hydrolytic cleavage and thus provide lignin its characteristic recalcitrance to degradation. Furthermore, due to its hydrophobicity and aromatic nature, lignin acts as an antimicrobial and waterproofing agent, protecting cellulose and hemicellulose from hydrolysis by microbial enzymes (Bugg & Rahmanpour, 2015; Hatti-Kaul & Ibrahim, 2013; Laurichesse & Avérous, 2014; Lourenço & Pereira, 2018; Ruíz-Dueñas & Martínez, 2009; Vanholme et al., 2010).

Lignin is constituted by three monolignols, or hydroxycinnamyl alcohols, as monomers, that differ in the degree of methoxylation, explicitly the non-methoxylated *p*-coumaryl alcohol, the monomethoxylated coniferyl alcohol and the dimethoxylated sinapyl alcohol (Figure 1.3 a). When these monolignols are incorporated into the lignin polymer, they give rise to three lignin type units, which are

p-hydroxyphenyl (H), guaiacyl (G) and syringyl (S), respectively (Bonechi et al., 2017; Vassão et al., 2008) (Figure 1.3 b).

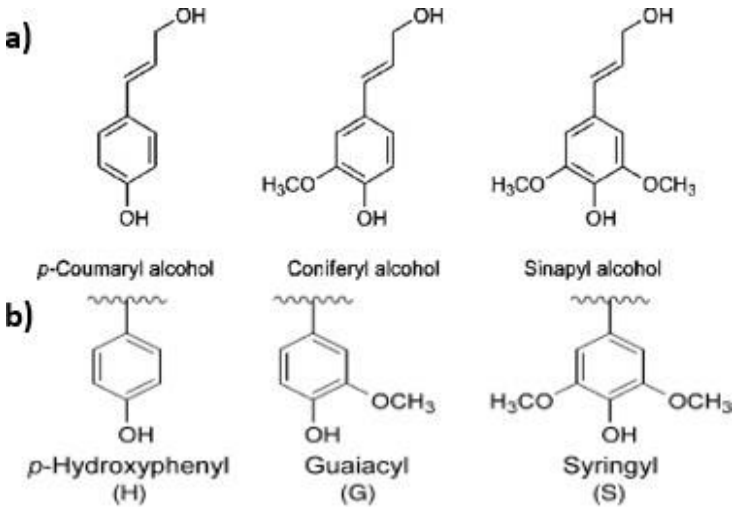

Figure 1.3: **a)** Lignin monolignols *p*-coumaryl, coniferyl and sinapyl alcohols. Adapted from Springob & Kutchan (2009) and **b)** lignin aromatic type units' *p*-hydroxyphenyl (H), guaiacyl (G) and syringyl (S). Adapted from Vassão et al. (2008).

Lignins are generally classified according to the chemical structure of their monomer units into three major groups, namely softwood lignin, hardwood lignin and grass lignin. Softwood lignin is predominantly produced from coniferyl alcohol, hardwood lignin (Figure 1.4) is composed from both coniferyl alcohol and sinapyl alcohol, whereas grass (Gramineae) lignin is produced from the three monomers. This lignin heterogeneity may be related to enzyme diversity among plant species and enzyme specificity regarding substrates (Lourenço & Pereira, 2018; Sjöström, 1993).

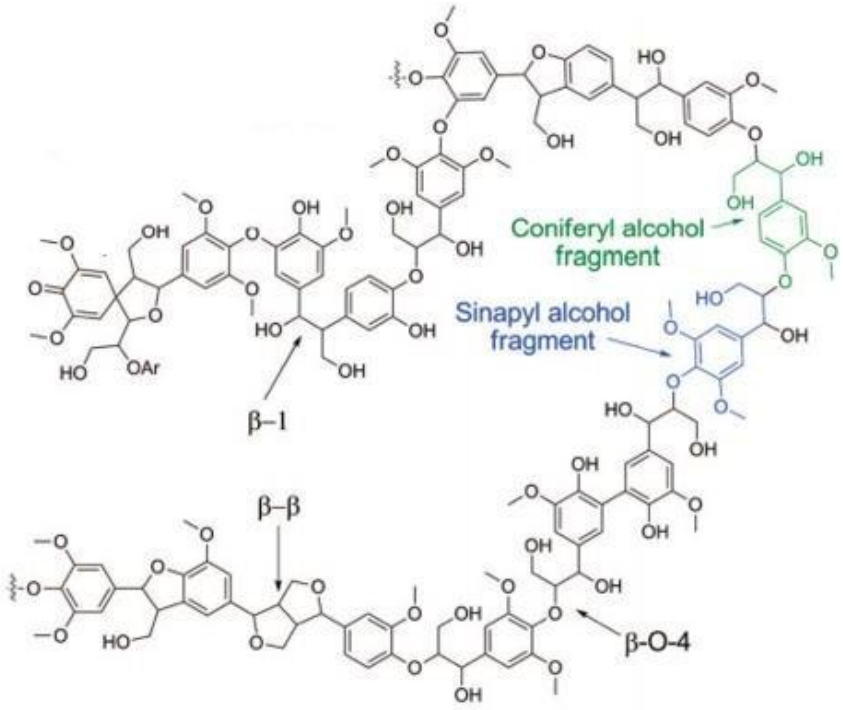

Figure 1.4: Schematic ilustration of a hardwood lignin structure. Adapted from Zakzeski et al. (2010).

The monolignols confer structural support, pathogen resistance and vascular integrity in plants and are biosynthesized in cytosol through the phenylpropanoid pathway. This pathway is also involved in the production of flavonoids, coumarins, lignans and anthocyanins (Fraser & Chapple, 2011; Vassão et al., 2008).

The pathway entry point is the amino acid phenylalanine, or tyrosine as a partial entry jointly with phenylalanine for some monocotyledons, which are derived from the shikimate pathway (Knaggs, 2003). The initial step is the formation of cinnamic acid from phenylalanine, through the action of the enzyme phenylalanine lyase (PAL). Cinnamic acid is then further converted in a multistep process to a variety of monolignols, including sinapyl, coniferyl and p-coumaryl alcohols (Abdelaziz et al., 2016).

After the biosynthesis, a monolignol is translocated to the apoplast of vascular and fiber cells by a mechanism that remains unclear. In that location takes place its oxidation, where the resulting radical is relatively stable due to delocalization of the unpaired electron in the conjugated system.

Consequently, the oxidized monolignol radical cross-couples with another monolignol radical, forming a dimer by a covalent bond between the two subunits (Vanholme et al., 2010). The oxidation of the lignin monomers involves peroxidases and/or laccases. Whereas laccases use oxygen, peroxidases use hydrogen peroxide (derived from apoplastic oxygen) as electron-acceptor substrate to oxidize the monolignols (Lourenço & Pereira, 2018; Vanholme et al., 2010). The polymerization of the monolignol radicals produces several interunit “nonphenolic” linkages in lignin, preferentially at their β positions, resulting essentially in the β-β, β-*O*-4, and β-5. The possible coupling products depend largely on the chemical nature of each of the monomers and the conditions in the cell wall, such as pH, ionic strength, monomer supply rate and enzymes’s specificity towards the three monolignols (Kishimoto et al., 2015; Tobimatsu & Schuetz, 2019; Vanholme et al., 2010). For the lignin polymer continue to grow, it needs to be oxidized again, to a radical, so another monolignol radical can couple on the free-phenolic end of the growing biopolymer. This mode of action, in which a monolignol radical adds to a growing biopolymer, is termed ‘end-wise’ polymerization, meaning that the biopolymer grows one monomer at a time (Tobimatsu & Schuetz, 2019; Vanholme et al., 2010). Lignin polymers are often terminated by a *p*-hydroxyl group, which is typically referred to as a “phenolic” group, or by connection to an additional lignin species (Sturgeon et al., 2013). Figure 1.5 demonstrates the assembly of the three lignocellulosic components after their synthesis.

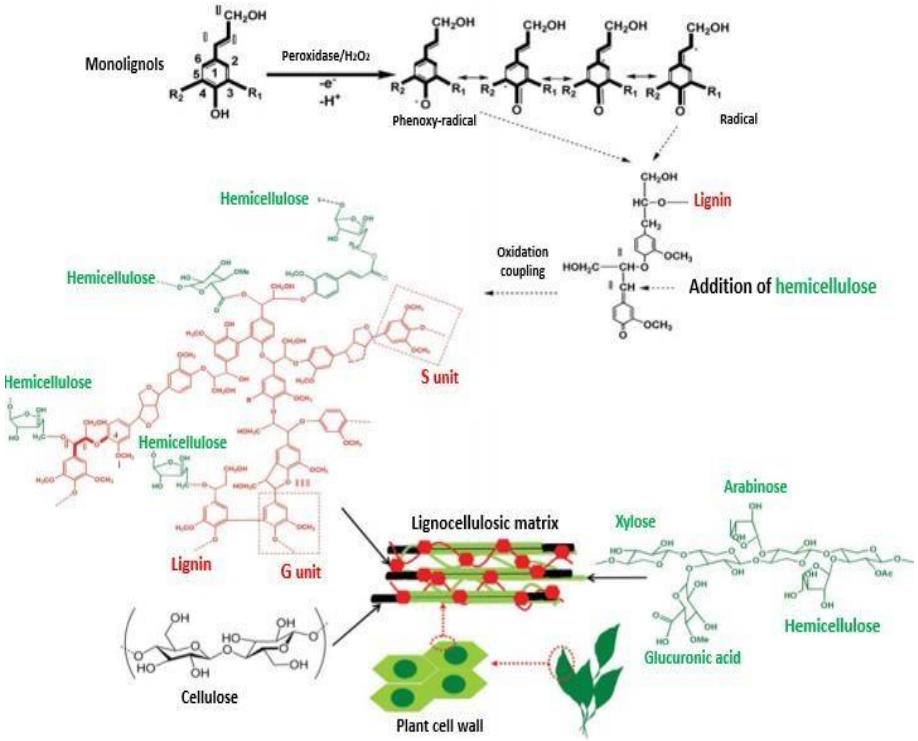

Figure 1.5: Simplified scheme of lignification, and composition of plant cell wall in a lignocellulosic matrix. Monolignols are oxidized by a peroxidase. Adapted from Monlau et al. (2013).

1.3 Lignocellulosic biorefinery

In a lignocellulose biorefinery operation, the feedstocks firstly need a pretreatment. The pretreatment step is mainly required for improving the accessibility of cellulose and hemicellulose by weakening the complex structure of lignin, enhancing the efficiency for further steps, while removing other minor components present in the lignocellulosic matrix (Kumar et al., 2009; Zakzeski et al., 2010). Next, the components are separated and degraded into their building blocks. The carbohydrate chains of cellulose and hemicellulose are disrupted by acidic or enzymatic hydrolysis, leading to sugars release. The sugar monomers are then biochemically converted into high-value products using fermentation by naturally occurring microorganisms to yield ethanol, acetic acid, higher alcohols or other compounds. Additionally, fuels can be recovered from the fermentation broth by separation/purification methods. The sugar units can also be converted through chemical conversion to yield 5-HMF, furan or formic acid (Figure 1.6) (Konwar et al., 2018; Kumar et al., 2009; Zakzeski et al., 2010).

Lignocellulosic biorefinery is currently limited due to technological constraints and high processing costs and it can only be considered an efficient and feasible process if it is able to separate cellulose, hemicellulose and lignin as efficiently as petrol refineries separate oil fractions. Furthermore, the extraction of these biomass components and their consequent valorization contributes for the economic viability and profitability of a biorefinery (Konwar et al., 2018; Ruíz-Dueñas & Martínez, 2009; Zakzeski et al., 2010).

Cellulose and hemicellulose have a large market in paper manufacture and production of fuels. Research and development activities towards these commercial products from both carbohydrates, opened a window for the valorization of lignin that is often considered as waste, being burned for energy supply. This poor usage of all components seriously affects the healthy development of lignocellulosic feedstock utilization, in fact only 2% of lignin was commercially used for production of low-value products. Valorization of lignin into high-value products, including carbon fibers, aromatic compounds, polymers, agrochemicals and fuel chemicals, is a key solution for overcoming techno-economical constrains of high operating costs of a lignocellulosic biorefinery (Konwar et al., 2018; Ruíz-Dueñas & Martínez, 2009; Ragauskas & Yoo, 2018; Shu et al., 2020). This broad range of products led to the common saying “You can make anything from lignin, except money” and, indeed, regarding lignin intrinsic structural features, its valorization is recently receiving considerable attention (Ragauskas et al., 2014; Strassberger et al., 2014; Zakzeski et al., 2010).

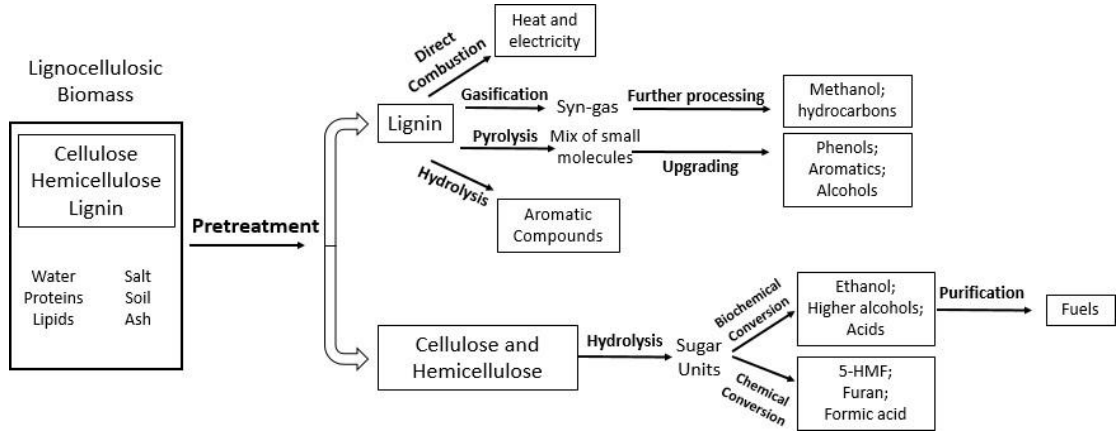

Figure 1.6: Simplified lignocellulosic biorefinery scheme. Cellulose and hemicellulose are integrated within lignin matrix, but it is not represented for simplicity. Adapted from Zakzeski et al. (2010).

To date, the difficulties in lignocellulosic biomass utilization and lignin valorization have centered mainly on lignin recalcitrance, which has always been a limitation in industrial (processing of wood in both pulp and paper manufactories) and natural (digestibility of pasturage by ruminants) processes (Bilal & Iqbal, 2020; Ruíz-Dueñas & Martínez, 2009; Shu et al., 2020; Vassão et al., 2008). This leads to a second hurdle, which is cellulose and hemicellulose cannot be readily converted into marketable products due to the recalcitrance of lignin, preventing accessibility of the carbohydrates (Ruíz-Dueñas & Martínez, 2009; Vassão et al., 2008). In fact, the structures of cellulose and hemicellulose are relatively simple, and both can be easily hydrolyzed by industrial processes into their sugar components and then be bio-transformed.

The solution encountered by industries for the so-called lignin challenge is in the pretreatment step (Ummalyma et al., 2019). Pretreatment should be carried out with minimal energy consumption and toxic by-products generation, with an optimal recovery of the components in shortened time and in an environmental friendly way (Chen, 2015; Jędrzejczyk et al., 2019). The existent pretreatment technologies for lignocellulosic biomass are physical, chemical and biological. The traditional physical pretreatment consists in an increase of temperature or pressure, causing changes in the lignocellulosic

cell wall and consequently reducing the biomass recalcitrance. Chemical pretreatment consists in the usage of organic or inorganic compounds that disrupt the linkages present in the lignocellulosic biomass cell wall. Both physical and chemical methods can be used individually or combined, increasing the yield of desired products. However, these methods require large inputs of energy and result in environmental pollution (Jedrzejczyk et al., 2019). In contrast, biological pretreatment consists in the application of microorganisms or enzyme cocktails directly on the feedstocks capable of degrading lignin. It is a selective process with low energy requirements, low severity and does not release toxic compounds to the environment and the by-products produced do not affect negatively the biorefinery process. Hence, from the three pretreatments, the biological is the most suitable for a green biorefinery. Since biological pretreatment strongly depends on enzymes, this technological approach demands a pre-search for appropriate microorganisms that cohabit with lignocellulosic materials and/or are capable of deconstruct lignin (Bugg et al., 2020; Ummalyma et al., 2019).

Microorganisms like fungi (white-, brown- and soft-rot fungi) and some bacteria from soil, manure, agricultural residues or the rumen of animals are known to produce lignin-degrading enzymes which show efficient delignification of lignin (Ummalyma et al., 2019; Zheng et al., 2017). Although fungi are more efficient microorganisms than bacteria for cell wall deconstruction because of their capability of producing larger amounts of enzymes and higher oxidative rates, fungal enzymes are more difficult to express in high yield for industrial applications. In addition, bacteria are simpler systems to study because of their higher growth rate, environmental adaptions, easiest gene cloning, heterologous expression, and versatile nature for their nutrients. Additionally, native biocatalysts may not have the robustness or enzymatic activity necessary for industrial applications and bacterial systems dispose of a greater number of commercially available molecular biology tools to improve their enzymatic properties (Kumar & Chandra, 2020). Moreover, bacterial biocatalysts benefit from higher optimal temperature, pH range, salt tolerance and stability compared with fungal enzymes. Hence, since 2010 lignin oxidizing enzymes from bacteria gained a resurgent interest (Bugg et al., 2020).

1.4 Identification and characterization of bacterial ligninolytic enzymes

In general, lignin-degrading enzymes can be divided in two main groups: lignin modifying enzymes (LMEs) and lignin-degrading auxiliary (LDA) enzymes. The first group includes laccases (benzenediol oxygen oxidoreductase; 1.10.3.2) and heme-containing peroxidases, in particular lignin (diarylpropane: oxygen, hydrogen-peroxide oxidoreductase; 1.11.1.14), manganese (Mn (II): hydrogen-peroxide oxidoreductase; 1.11.1.13), versatile (Reactive black-5: hydrogen-peroxide oxidoreductase; 1.11.116) and dye decolorizing peroxidase (Reactive-Blue-5: hydrogen-peroxide oxidoreductase; 1.111.19). The second group comprises enzymes such as cellobiose dehydrogenase (cellobiose: acceptor 1-oxidoreductase; 1.1.99.18), aryl-alcohol oxidase (aryl-alcohol: oxygen oxidoreductase; 1.1.3.7) and glucose oxidase (β-D-glucose: oxygen 1-oxidoreductase; 1.1.3.4) (Hatti-Kaul & Ibrahim, 2013; Janusz et al., 2017; Kumar & Chandra, 2020).

LMEs are more suitable for industrial applications since their oxidation reactions towards aromatic substrates allow depolymerization of lignin through cleavage of carbon-carbon and ether

interunit bonds, whereas LDA enzymes are not capable of depolymerize lignin without involvement of LMEs. Furthermore, LDA enzymes are mostly found in white-rot fungi secretomes, while peroxidases are generally found in microbes, bacteria, insects, plants, fungi and animals, and laccases are mainly obtained from bacteria, insects, plants and fungi (Hatti-Kaul & Ibrahim, 2013; Janusz et al., 2017; Morsi et al., 2020). Laccases, in contrast to peroxidases, are less selective and characterized by the readily ability to use molecular oxygen as electron acceptor, instead of hydrogen peroxide, with only production of water as byproduct, which increase laccases' biotechnological applications and are, therefore, more suitable at an industrial scale. Indeed, they are one of the most important, studied and identified prokaryotic copper-activated ligninolytic enzymes, belonging to a family of enzymes named multicopper oxidases (Hatti-Kaul & Ibrahim, 2013; Janusz et al., 2017; Jaufurally et al., 2016; Martins et al., 2015).

1.4.1 Multicopper oxidases

Multicopper oxidases (MCOs) are multifunctional enzymes found in the genome of the three Domains of Life (Archaea, Bacteria and Eukarya) and have important metabolic roles in delignification, lignification, morphogenesis, copper homeostasis and protection against UV light and hydrogen peroxide (Giardina et al., 2010; Martins et al., 2015).

MCOs are a family of enzymes that contain approximately 500 amino acid residues and are composed of three Greek key β-barrel cupredoxin domains (domains 1, 2 and 3) (Figure 1.7). Structurally, MCOs contain at least four copper atoms that are responsible for the redox reactions. The typical copper content of MCOs includes one type-1 Cu (II) (T1Cu) located at domain 3 and one type-2 (T2Cu) along with two type-3 Cu (T3Cu) (II) arranged in a trinuclear cluster (TNC) between domains 1 and 3 (Giardina et al., 2010; Jones & Solomon, 2015; Martins et al., 2015). Type 1 Cu (II) site comprises two histidine ligands and one cysteine arranged in a distorted trigonal geometry around the copper ion. In some laccases a methionine axial ligand, attribute a tetrahedral geometry to the site. Due to the copper-cysteine linkage in type 1 Cu (II) site, this copper ion is known as "blue copper" because this bond leads to an intense absorption around 600 nm. The trinuclear cluster comprise type 2 copper (T2) and the binuclear type 3 copper (T3) sites. The T2 Cu is coordinated by two histidine residues and one water molecule, exhibiting weak absorption in the visible region and is close to the binuclear T3 copper sites, which are coordinated by three histidine residues and show a strong absorption band at 330 nm. MCOs couple four single-electron oxidations of the reducing substrate to the reduction of molecular oxygen to water. T1 Cu ion acts as the primary acceptor of electrons from the substrate. The four electrons are subsequently transferred through a His-Cys-His tripeptide to the trinuclear cluster, where occurs the reduction of oxygen, in two molecules of water (Borges et al., 2020).

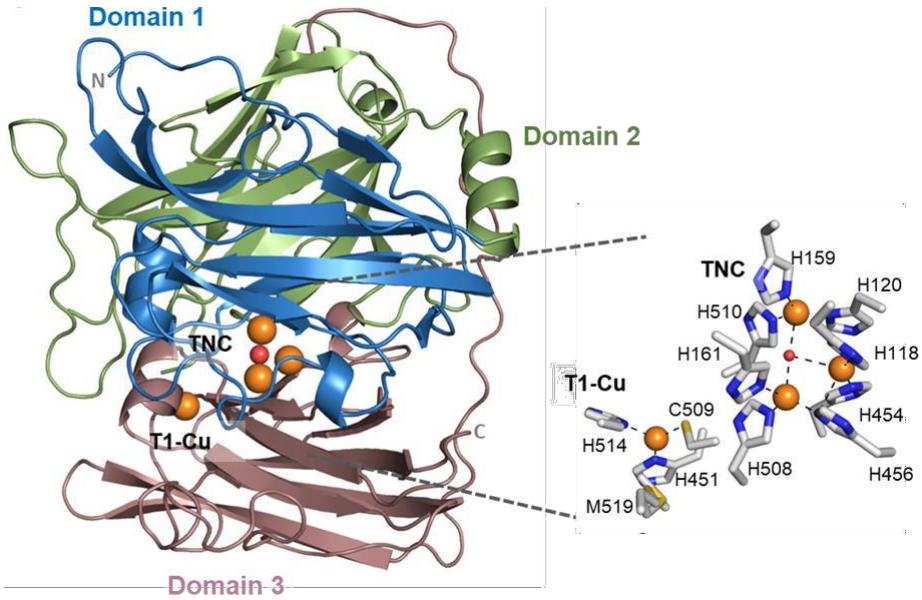

Figure 1.7: Overall crystal structure of McoA from *Aquifex aeolicus*. Domain 1, 2 and 3 are coloured as blue, green and brown, respectively. T1Cu site is located in domain 3 and TNC is located in the interface between domain 1 and 3. The coppers atoms are represented as orange spheres. **Highlight** Representation of the T1Cu and TNC site from wild type McoA. The copper ligands are represented as sticks with carbon, nitrogen, oxygen and phosphorous atoms in grey, blue, red and orange, respectively. The oxygen atom is represented as a red sphere. Adapted from Borges et al. (2020).

Although MCOs are a family of enzymes with similar three-dimensional organization that catalyze the oxidation of substrates by using molecular dioxygen as electron acceptor, their substrate specificity and amino acid sequence composition varies within the family members. As such, MCOs are divided into two functional classes: metallo-oxidases (EC 1.16.3) that oxidize low valence metal ions with higher efficiency as compared with organic substrates and laccases that oxidize bulkier compounds (Martins et al., 2015) with higher efficiency than metal ions.

1.4.1.1 Bacterial metallo-oxidases

Metallo-oxidases have notable catalytic efficiency (k_{cat}/K_m) against low-valent metallic ions, such as copper (Cu^{2+}), iron (Fe^{2+}) or manganese (Mn^{2+}). Prominent metallo-oxidases such as CueO from *Escherichia coli*, yeast ferroxidase Fet3p and human ceruloplasmin, are known to be involved in metal homeostasis mechanisms of the respective organisms (Fernandes et al., 2007; Kosman, 2002; Jones & Solomon, 2015; Martins et al., 2015).

The majority of metallo-oxidases are characterized by the presence of a methionine-rich loop (Met-loop) blocking the access to T1 copper site (Martins et al., 2015). The putative smaller substrate binding pocket of these enzymes seems in accordance to their preference for the oxidation of small metal ions (Fernandes et al., 2010; Silva et al., 2012; Singh et al., 2004). Accordingly, one reason for the lower specificity towards bulkier compounds, like the phenolic units from lignin, can be due to steric hindrance in the binding close to the T1 Cu binding site (Martins et al., 2015; Silva et al., 2012). The Met-loops close to this catalytic centre vary in length, composition and structure and have been proposed to bind copper and interact with other proteins involved in copper trafficking and homeostasis,

however, the mechanistic features of Met-rich segments in MCOs are largely unknown (Borges et al., 2020).

Aquifex aeolicus is a microaerophilic oxygen-respiring microorganism that habits volcanically heated habitats. This is one of the most thermophilic bacteria known, and expresses McoA, a thermoactive and thermostable MCO, which is presumably involved in the protein's response to copper and iron toxicity. McoA has an optimal temperature of 75°C and presents remarkable heat stability at 80 and 90°C, with activity lasting for up to 9 and 5 h, respectively. Considering its enhanced thermostability, this enzyme is worthwhile considered exploring for biotechnological applications. However, it exhibits a higher catalytic efficiency for cuprous and ferrous ions oxidation as compared to aromatic substrates, (Borges et al., 2020; Fernandes, 2007; Fernandes et al., 2009). McoA has a 29-residue long loop, with 12 methionines, putatively close to the T1 Cu site but absent from the crystal structure (Borges et al., 2020). Recent results show that the Met-loop in McoA is capable of controlling access of substrates to the catalytic site and determining the chemical environment of the T1-Cu center revealing a gating role in McoA (Borges et al., 2020).

1.4.1.2 Bacterial laccases

Most laccases isolated within the Bacteria domain were isolated from the *Bacillus* and *Streptomyces* genera despite the report of laccase activity in some other bacterial species (Martins et al., 2015). CotA laccase from *Bacillus subtilis*, found at its endospores, is the most extensively studied bacterial laccase both from the fundamental and applied point of view (Martins, 2002, 2015). The endospore is constituted by a multi-layered protein coat, where CotA is localized, more specifically, in the surface layers, being responsible for the characteristic brown melanin-like pigment of the endospore which offers protection against stresses. Moreover, CotA is responsible for oxidative cross-linking of other endospore coat structural components and is characterized by a high thermal stability with an optimum temperature of 75°C (Henriques & Moran, 2000; Martins et al., 2002). In contrast with metallo-oxidases, CotA-laccase has a more accessible catalytic T1 Cu site with apolar amino acids. Even compared to some other bacterial laccases, CotA seems to have a broader substrate binding site close to T1 Cu site, resulting in an increased accommodation for bulkier compounds (Martins et al., 2002, 2015).

Laccases' typical substrates are *ortho*- and *para*- diphenols, aminophenols, polyphenols and polyamines because their redox potential are low enough to allow electron abstraction by the type 1 copper ion, whereas substrates characterized by high redox potential cannot be directly oxidized by bacterial laccases. Nonetheless, due to their wide range of reducing substrates, bacterial laccases are considered the most promising ligninolytic enzymes for lignocellulose biorefineries and, as a consequence, a target of intense study (Giardina et al., 2010; Jones & Solomon, 2015; Martins et al., 2015).

1.5 Bacterial laccases limitation for lignin depolymerization and valorization

Phenolic units of lignin have low redox potential (0.5-0.8 V *vs.* NHE range) (Calcaterra et al., 2008) and thus, are redox compatible with, for instance, CotA-laccase that has a relatively low redox potential (0.525 V *vs.* SHE) (Durão, 2008b). However, these phenolic moieties correspond only to 10-20% of lignin, while the remaining 80-90% correspond to non-phenolic units, which have redox potentials above 1.3 V. Moreover, non-phenolic units act as steric hindrance for phenolic units, reducing enzyme accessibility towards them. Thus, it is vital to understand how to efficiently remove these non-phenolic fractions for lignin valorization (Konwar et al., 1999).

The oxidation of these non-phenolic substrates becomes possible in the presence of redox mediators that, when oxidized by laccases, turn into reactive phenoxy-radicals capable of overcoming redox restrictions (Figure 1.8) (Calcaterra et al., 2008; d'Acunzo & Galli, 2003; Rosado et al., 2012).

Figure 1.8: Catalytic cycle of a laccase-mediator system. Adapted from d'Acunzo & Galli (2003).

Usually these laccase mediator systems (LMSs) rely on synthetic mediators like 2, 2'-azinobis (3-ethyl-benzothiazoline-6-sulfonic acid) (ABTS) or violuric acid that are expensive and may generate toxic species (Pardo & Camarero, 2015), therefore natural mediators are the preferable option. Several studies (Camarero et al., 2005; Camarero et al., 2008; Rosado et al., 2012) have shown that natural phenolic compounds present in lignin's structure are capable of acting as electron mediators with improved performances compared with synthetic mediators and are presumably directly involved in the degradation of lignocellulose biomass by fungi and bacteria in nature. The natural phenolic mediators seem to be grouped in three families, or types, of phenolics, syringyl-, guaiacyl, and hydroxyphenyl-type. For this work were selected the monolignols 2,6-dimethoxyphenol (2,6-DMP), sinapyl alcohol, sinapic acid, acetosyringone, syringaldehyde and methylsyringate of the syringyl-type, the guaiacyl-type's guaiacol, coniferyl alcohol, coniferyl aldehyde ferrulic acid and vanillin and, finally, caffeic acid and *p*-coumaric acid of the hydroxyphenyl-type.

Laccases are involved in the first steps of lignin biosynthesis by oxidative phenolic coupling and in the opposite action which is the oxidative degradation of lignin, mostly by auxiliary of a phenolic compound as mediator. Industries have taken advantage of the former process for obtaining dimers or oligomers of these monolignols with antifungal properties (Nemadziva et al., 2018), medical uses or for material synthesis (Jaufurally et al., 2016).

1.6 Turning a metallo-oxidase into a laccase by directed evolution

Due to their robustness and high thermal stability, extremophile MCOs, such as McoA from *Aquifex aeolicus*, are promising enzymes for lignocellulose biorefinery pretreatment however, it is crucial that this enzyme shows high catalytic efficiency for aromatic compounds, i.e. phenolics.

With the rapid development of structural biology, a large amount of progress was made in protein engineering approaches. One of these is directed evolution that modifies protein features or functions by redesign protein structures at a molecular level. Performing enzyme directed evolution requires simulating in laboratory the principles of natural selection through iterative rounds of random mutagenesis, generating mutant libraries from which vast numbers of variant enzymes are screened in high-throughput assays for identification of the variants with a desired structure or function. The most frequently used technique of random mutagenesis is error-prone Polymerase Chain Reaction (epPCR) that consists in a deficient proof-reading DNA polymerase ability for a low fidelity polymerase chain reaction. This technique results in several errors in the gene sequence leading to alterations in the codified amino acid sequences (Brissos et al., 2015; Kwan, 2017; Martins et al., 2015; Zhang et al., 2020).

Thus, tailoring the McoA metallo-oxidase by directed mutagenesis into a novel enzyme with a CotA-alike activity, besides constituting a major advantage for interesting products synthesis and for a lignocellulosic biorefinery, it is also a means to understand the structural features responsible for the substrate specificities of both enzymatic classes from the same family (Martins et al., 2015). Brissos et al. (2015) described a laboratory directed evolution of the recombinant hyperthermostable metallo-oxidase McoA, expressed in a recombinant strain of *E. coli*, into an improved variant selected on the basis of its higher ABTS enzymatic activity (Figure 1.9). The purified variant McoA 2B3 showed a 100-fold increase in the oxidation rate of ABTS, reaching a catalytic efficiency comparable to CotA-laccase.

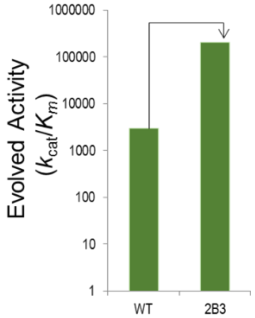

Figure 1.9: Comparison between catalytic efficiencies between McoA and the McoA variant 2B3 towards ABTS. The variant showed a 100-fold increase in the oxidation rate of ABTS.

The 2B3 variant (10 mutations) was further evolved on the basis of increased enzymatic activity towards 5h3 monolignol 2,6-DMP (Figure 1.10, results not published). First, a back DNA-shuffling, in which the genes of McoA wild-type and 2B3 were randomly reassembled through PCR, lead to the selection of 22B7 variant with only 4 mutations but with a similar activity towards ABTS as 2B3. The catalytic efficiency towards 2,6-DMP was very low (50 $M^{-1} \cdot s^{-1}$). Four rounds of mutagenesis followed by screening generated 1B9 variant. Next, the 43-residue peptide sequence was removed followed by a new back-DNA shuffling with wild-type gene to reduce the number of non-beneficial mutations, leading to hit 15E6. The long Met-rich loop was removed from 15E6 variant, resulting in 15E6-loop5 (loop with 5 residues) variant. This variant was used as parent in a new round of mutagenesis using epPCR resulting in variant 23B3 exhibiting approximately 1000-fold increase catalytic efficiency when compared to 22B7 (Figure 1.10).

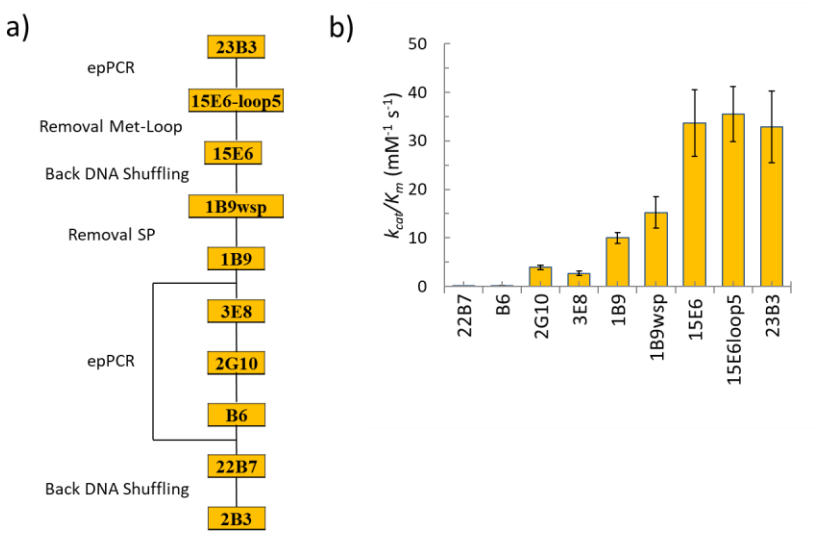

Figure 1.10: (a) Lineage of McoA variants generated during evolution to increase enzymatic activity towards monolignol 2,6-DMP and (b) k_{cat}/K_m for the oxidation of 2,6-DMP in McoA variants.

1.7 Scope of the present thesis

In this work, recombinant McoA 15E6-loop5 and McoA 23B3, as well as CotA-laccase, were produced in *E. coli* cells, purified using well-established chromatographic techniques, and characterized. Their kinetic properties towards a set of lignin-related phenolic substrates, syringyl-, guaiacyl- and hydroxyphenyl-type was assessed. The aim was to evaluate if the engineered McoA enzymes have extended activity apart from 2,6-DMP, the substrate that was used during the screenings of directed evolution. Furthermore, the idea was to compare these activities to those of the well-established CotA-laccase. This evaluation would allow to eventually secured (in case comparable activities were achieved) new hyperthermophilic bacterial laccases leading to an enhancement of the range of ligninolytic enzymes for lignocellulose biorefinery and for industrial processes for interesting products synthesis. Indeed our results showed that for the majority of substrates tested the McoA variants showed similar k_{cat}/K_m values to CotA. Overall, 15E6-loop5 exhibited slightly improved performance than 23B3 variant.

Bioconversion reactions at a large scale were tested with the most promising substrates, namely sinapyl alcohol, coniferyl alcohol and caffeic acid, towards the synthesis of added-value products, syringaresinol (Jaufurally et al., 2016), pinoresinol (Wan et al., 2007) and phenyllinsin A (Nemadziva et al., 2018), respectively (Fig 1.11). Reactions using coniferyl alcohol and caffeic acid did not result in the desired product but we were able to optimize reactions that resulted in similar or higher yields of syringaresinol from sinapyl alcohol as obtained in bioprocesses with peroxidases (Ozawa et al., 2014) and fungal laccases (Jaufurally et al., 2016). Reactions were first optimized using CotA-laccase and then compared to engineered McoA15E6-loop5 variant, where the quantity of syringaresinol production were lower.

These results have stimulated further evolution of McoA by epPCR directed evolution using a less unbiased polymerase than Taq DNA polymerase, Mutazyme II, in order to continue the lineage of

McoA variants with laccase-alike activity. This work was interrupted because of the COVID-19 outbreak and only validation studies were performed.

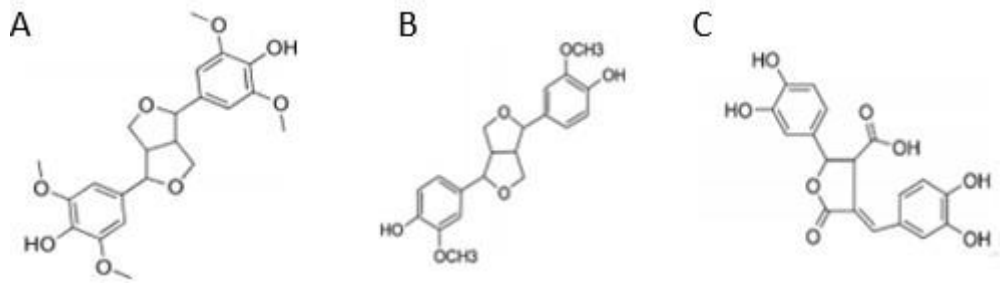

Figure 1.11: Structure of syringaresinol (A), pinoresinol (B), and phellinsin A (C).

.

2. Materials and Methods

2.1 Bacterial strains, plasmids and culture media

The bacterial strain used for expression of *cotA*, and *mcoA* variants was *E. coli* Tuner ΔcueO::kan (DE3) in which the *cueO* gene, that codes for the multicopper oxidase CueO, was replace by a kanamycin resistance gene. The protein genes were cloned in pET-21a(+) plasmid, controlled by the T7 promotor and induced by isopropyl β-D-1-thiogalactopyranoside (IPTG). The plasmids used for CotA, McoA 15E6-loop5 and McoA 23B3 expression were pLOM10 (Martins et al., 2002), pMcoA15E6-loop5 and pMcoA23B3, respectively. The media used was Luria-Bertani (LB) medium with the following composition (per liter of distilled water): 10 g of tryptone; 10 g of sodium chloride and 5 g of yeast extract. Terrific Broth (TB) medium with salts was used with the following composition (per liter of distilled water and per 100 mL of distilled water, respectively): 12 g tryptone, 24 g of yeast extract, 4 mL Glycerol (86 %), 900 mL H_2O; 2.3 g KH_2PO_4, 12.5 g K_2HPO_4, 100 mL H_2O. LB with agar (LA) medium was used with the following composition (per liter of distilled water): 10 g of tryptone 10 g of sodium chloride; 5 g of yeast extract and 15 g of agar. LB, LA and TB mediums were used for the growth and maintenance of *E. coli* Tuner ΔcueO::kan, supplemented with the appropriate antibiotics when necessary.

2.2 Cell transformation

One or five microliters of purified plasmids or ligation mixtures, respectively, were added to an aliquot of 100 µL electrocompetent *E. coli* Tuner ΔcueO::kan cells (previously thawed on ice) mixed and placed on ice for 5 min. This mixture was transferred to a sterile and ice-cold electroporation cuvette, which was placed in the Xcell ShockPod chamber (Gene Pulser Xcell, Biorad) and pulsed using set conditions C = 25 µF, PC = 200 Ω, V = 2.5 kV. Cells were immediately suspended in 1 mL of LB and incubated at 37ºC and 170 rpm, during 1 h. Cells were then centrifuged (5,000 rpm during 5 min) and the culture was plated on LA Petri dishes supplemented with ampicillin (100 µg/L) and kanamycin (10 µg/L). The Petri dishes were incubated overnight at 37ºC.

2.3 Bacterial growth

2.3.1 Pre-inoculum

Pre-inoculum was prepared by inoculating a single colony in 50 mL of LB medium supplemented with ampicillin (100 µg/mL) and kanamycin (10 µg/mL) in a 250 mL Erlenmeyer. The pre-inoculum was incubated at 37ºC and 170 rpm, overnight.

2.3.2 Growth

Bacterial growth was performed in a 5 L Erlenmeyer with 1 L of LB medium, supplemented with ampicillin (100 µg/mL) and kanamycin (10 µg/mL). A volume of pre-inoculum was added in order to start the growth with an optical density at 600 nm (OD_{600}) of 0.05. The culture was incubated at 37ºC at 170 rpm, and bacterial growth was monitored by measuring the OD_{600}. At OD_{600} ~ 0.8, 0.1 mM IPTG and 0.25 mM $CuCl_2$ were added for gene expression induction and lead to full protein incorporation of Cu ions. The agitation was stopped 4 h after induction, since cells accumulate higher amounts of Cu under

microaerobic growth conditions (Durão, 2008a), and cells were incubated static at 25°C, overnight. After 24 h, cells were harvested by centrifugation (18,000*g* at 4ºC during 10 min) and the pellets were washed NaCl 0.9% (w/v). Cells were centrifuged and stored at -20ºC.

2.4 Protein purification

2.4.1 Buffer solutions

For the protein purification steps, the following buffers were used: 20 mM Tris-HCl at pH 7.6 (Buffer A); 20 mM Tris-HCl with 1 M NaCl at pH 7.6 (Buffer B) and 20 mM Tris-HCl with 0.2 M NaCl at pH 7.6. Buffer solutions were filtered and deoxygenized with a Millipore Membrane Filter 0.22 µm pore size using a vacuum filtration system.

2.4.2 Cells disruption

Cell pellets resultant from 2.3.2 were re-suspended with 5 mL of Buffer A, 1 µL/mL of DNase I (stock 1U/mL), and 2 µL/mL of a mixture of protease inhibitors, antipain and leupeptin (stock 1 mg/mL) and 5 µL/mL of $MgCl_2$ (stock 1 M). Cells were disrupted using a French Press (Thermo EFC), operating at 1000 psi in a process repeated 3 times and lysates were centrifuged (40,000*g* at 4ºC for 2 h). Cell crude extracts (supernatants) were incubated at 80ºC during 20 min. The thermal denatured proteins were removed by centrifugation (12,000*g* for 10 min) and the supernatants (cell crude extracts) were filtered using a Millipore Membrane Filter 0.22 µm pore size.

2.4.3 Protein purification using an ÄKTA Purifier

2.4.3.1 Ion-exchange chromatography

For CotA the supernatant mentioned in 2.4.2 was loaded onto an ion-exchange SP-sepharose column (GE Healthcare) equilibrated with Buffer A, while for McoA variants the supernatant was loaded onto a Q-Sepharose column (GE Healthcare) equilibrated with Buffer A. Proteins were eluted in a two-step linear NaCl gradient (0.0 - 0.5 and 0.5 - 1 M) with Buffer B at a flow rate of 5.0 mL/min. The collected fractions were assayed for activity with ABTS 1 mM and 100 mM acetate buffer, pH 4.0, and the active fractions were visualized by sodium dodecyl sulfate polyacrylamide gel electrophoresis (SDS-PAGE). Fractions that showed bands with 35 and 65 kDa were collected, pooled and concentrated using an Amicon centriprep with a membrane with a cutoff 30 kDa.

2.4.3.2 Size-exclusion chromatography

The concentrated fraction was loaded onto a Superdex 200 HR 10/30 column (GE Healthcare) equilibrated with 20 mM Tris-HCl buffer, pH 7.6, 0.2 M NaCl, at a flow rate of 1.0 mL/min. Fractions were assayed for activity with ABTS 1 mM and 100 mM acetate buffer, pH 4.0, and the active fractions visualized by SDS-PAGE. The fractions containing purified enzymes were pooled, aliquoted and stored at -20°C. Enzyme concentration was measured using Bradford method and the Abs_{280nm} value, as mentioned in 2.6.

2.5 SDS-Page analysis

Fractions selected in 2.4.3.1 (20 µL) and 2.4.3.2 (15 µL) were added to 2 µL of loading buffer (0.7% 2-mercaptoethanol in 0.5 M Tris with 0.4% SDS, pH 6.8, 50% glycerol, 10% SDS, and 0.5% bromophenol blue) and boiled at 100ºC for 20 min and spin-down at 12,000*g*. These samples and 5 µL of protein molecular weight marker Precision Plus Protein Unstained Standard (Bio-Rad) were loaded into a 12.5 % SDS-PAGE and a charge of 220 V was applied during 45 min. The gel was then stained with a staining solution (0.25% Coomassie Brilliant Blue G-250, 45% Ethanol, 10% Acetic Acid) during 30 min and distained with a distaining solution (30% ethanol and 70% acetic acid). A 12.5 % SDS-PAGE with 2 µg of protein from each the three purification steps was also performed.

2.6 Protein quantification

The protein concentration was measured by using the absorbance band at 280 nm or the Bradford assay (Bradford, 1976) using bovine serum albumin as standard.

2.6.1 Protein quantification by Bradford method

Protein quantification by Bradford method was performed using Bradford reagent (0.005% Coomassie Brilliant Blue G-250, 5% methanol and 10% phosphoric acid) and bovine serum albumin (BSA) aliquots at different concentrations: 0.05, 0.1, 0.15, 0.2, 0.25, 0.3, 0.35, 0.4, 0.45, 0.5, 0.55 and 0.6 mg/mL. The calibration curve of absorbance at 595 nm versus BSA concentrations (Figure S1) was constructed by adding 10 µL of BSA at the different concentrations (10 µL of water for the blank) to 200 µL of Bradford reagent in a 96-well plate (triplicates). The 96-well plate was kept at room temperature for 10 min and then the absorbance at 595 nm was measured. The values were expressed as the mean of triplicate experiments. Protein was quantified by adding 10 µL of the protein to 200 µL Bradford reagent and measuring the absorbance at 595 nm. Protein concentration was determined by using the equation obtained in the calibration curve.

2.6.2 Protein quantification by Abs_{280nm} method

The purified protein concentration was determined using equation 1. The extinction coefficient values at 280 nm are 75,875 M^{-1} cm^{-1} for McoA and 84,739 M^{-1} cm^{-1} for CotA proteins.

$$[\text{Protein}] = \frac{\text{Abs at} 280\text{nm}}{\varepsilon\ 280\text{nm(protein)}} \qquad \text{Equation 1}$$

The resultant value from Equation 1 can be converted from M^{-1} cm^{-1} into mg/mL by dividing the value with the optical path length (1 cm) and multiplying the protein molecular weight (1 Da = 1 g/mol) in mg/mol (65 kDa for CotA and 57.8 kDa for McoA proteins).

2.7 UV-Visible spectra

UV-visible absorption spectra of purified enzymes were obtained at room temperature using a Nicolet Evolution 300 spectrophotometer from Thermo Industries using a cuvette with 1 cm optical path

length. Buffer 20 mM TrisHCl buffer, 0.2 M NaCl, pH 7.6 was used as blank and the assay was performed in triplicate.

2.8 Copper quantification

The copper content was determined by the bicinchoninic acid (BCA) method using $CuCl_2$ as a standard (Brenner & Harris, 1995). Reagent A, reagent B and reagent C were used with the following composition: Reagent A (30 g of TCA in 100 mL of distilled water); Reagent B (35.2 g of L-dehydroascorbic acid in 100 mL of distilled water); Reagent C (6 mg of purified bicinchonic acid disodium salt recrystallized powder, 3.6 g of NaOH, 15.6 g of N [12-hydroxyethyl] piperazine-N'-[2-ethane-sulfonic acid] sodium salt with 90 mL of distilled water).

The calibration curve (Figure S2) was constructed using $CuCl_2$ aliquots at different concentrations: 5, 10, 15, 20, 25, 30, 35, 40, 45 and 50 µM. The assay was performed in triplicate. In 2 mL Eppendorf tubes were added 0.75 mL of each copper aliquots at different concentrations (0.75 mL of Buffer A as blank) and 0.25 mL of reagent A. The tubes were centrifuged at 12,000*g* for 5 min. A volume of 0.5 mL of the supernatant was transferred to a cuvette where were added 0.1 mL of reagent B and 0.4 mL of reagent C. The mixture was mixed and the absorbance was read at 354.5 nm and the calibration curve (absorbance at 354.5 nm versus copper concentrations) was constructed.

Copper quantification was determined using equation 2:

$$\frac{[\mathrm{CuCl2}]\ (\mathrm{M})}{[\mathrm{Protein}](\mathrm{M})} \qquad \text{Equation 2}$$

Where $[CuCl_2]$ corresponds to the concentration of copper in the protein that is determined using the equation obtained by the calibration curve, and [Protein] ($Conc_{final}$) corresponds to the concentration of protein in the 0.75 mL ($Volume_{initial}$) added to the cuvette in 1 mL ($Volume_{final}$), calculated using equation 2.1:

$$Conc_{initial} \times Volume_{initial} = Conc_{final} \times Volume_{final} \qquad \text{Equation 2.1}$$

Where $Conc_{initial}$ is the protein concentration value determined either by the calibration curve obtained by Bradford method (2.6.1) or by Equation 1 through Abs_{280nm} method (2.6.2).

2.9 UV-Visible spectra of phenolic compounds

The UV-Visible spectra of lignin related phenolic compounds were recorded in 0.1 M phosphate buffer, pH 8.0 in the wavelength range 300-800 nm using either a Nicolet Evolution 300 spectrophotometer from Thermo Industries (Waltham, MA, USA) or a Synergy 2, Biotek, microplate reader.

2.10 Molar extinction coefficients (ε) of phenolic compounds

The molar extinction coefficients of coniferyl alcohol, vanillin, caffeic acid and *p*-coumaric acid were determined by measuring their maximal wavelengths at pH 4.0 and pH 8.0 (in concentrations 5, 20, 40, 80, 150, 200 and 250 µM) using the Lambert-Beer law ($A = \varepsilon \times l \times c$; where A is the absorbance,

l the optical length (0.65 cm) and c the compound concentration) using a Synergy 2, Biotek, 96-well microplate reader (Figure S3). The values are result of triplicates.

2.11 Steady-state kinetics of phenolic compounds

The optimal pH values were determined using Britton Robinson buffer (100 mM phosphoric acid, 100 mM boric acid and 100 mM acetic acid mixture with 0.5 mM NaOH to the desired pH), at a pH range between 3.0 and 12.0. Initial rates of oxidation of the chemical compound ABTS and of the lignin related phenolics 2,6-DMP, sinapyl alcohol, syringaldehyde, acetosyringone, methylsyringate guaiacol, coniferyl aldehyde, coniferyl alcohol, caffeic acid, sinapic acid, vanillin, *p*-coumaric acid and ferulic acid were monitored at room temperature using a Nicolet Evolution 300 spectrophotometer at appropriate wavelengths. The kinetic parameters were measured at 25°C in 100 mM sodium acetate buffer, pH 4, for CotA towards ABTS (0.5 – 1 mM) and sodium acetate buffer, pH 6, for McoA variants towards ABTS (0.1 – 25 mM), and in 100 mM potassium phosphate, pH 8, for the lignin-related phenolics 2,6-DMP (0.02 – 5 mM, pH 8), guaiacol (0.02 – 3.5 mM, pH 8, for CotA and 0.02 – 25 mM, pH 8, for McoA variants), and for the other lignin-related phenolics (0.0075 - 0.5 mM, pH 8). Reactions were followed at 420 nm (ε_{ABTS} = 36,000 $M^{-1} \cdot cm^{-1}$), 468 nm ($\varepsilon_{2,6\text{-}DMP}$ = 49,600 $M^{-1} \cdot cm^{-1}$) (values referent to 2,6-DMP's reaction product), 275 nm ($\varepsilon_{Sinapyl\ alcohol}$ = 5,738 $M^{-1} \cdot cm^{-1}$), 310 nm ($\varepsilon_{Sinapic\ acid}$ = 16,000 $M^{-1} \cdot cm^{-1}$), 360 nm ($\varepsilon_{Syringaldehyde}$ = 16,000 $M^{-1} \cdot cm^{-1}$), 360 nm ($\varepsilon_{Acetosyringone}$ = 12,000 $M^{-1} \cdot cm^{-1}$), 320 nm ($\varepsilon_{Methylsyringate}$ = 12,461 $M^{-1} \cdot cm^{-1}$), 470 nm ($\varepsilon_{Guaiacol}$ = 49,600 $M^{-1} \cdot cm^{-1}$) (values referent to guaiacol's reaction product), 350 nm ($\varepsilon_{Coniferyl\ aldehyde}$ = 14,938 $M^{-1} \cdot cm^{-1}$), 265 nm ($\varepsilon_{Conyferyl\ alcohol}$ = 9,697 $M^{-1} \cdot cm^{-1}$), 310 nm ($\varepsilon_{Ferrulic\ acid}$ = 13,092 $M^{-1} \cdot cm^{-1}$), 340 nm ($\varepsilon_{Vanillin}$ =12004 $M^{-1} \cdot cm^{-1}$), 320 nm ($\varepsilon_{Caffeic\ acid}$ = 11,310 $M^{-1} \cdot cm^{-1}$), 290 nm ($\varepsilon_{p\text{-}Coumaric\ Acid}$ = 17,560 $M^{-1} \cdot cm^{-1}$). The values were expressed as the mean of triplicate experiments. Kinetic data was fitted directly using the Michaelis-Menten equation (Origin-Lab, Northampton, MA, USA)). The protein concentration was measured by using the Bradford assay or Abs_{280nm} method, as mentioned in 2.6. One unit of laccase activity was designated as the quantity of laccase capable of oxidizing 1 µmol of substrate per minute.

2.12 Scale-up reactions

2.12.1 Preliminary reactions using sinapyl alcohol, coniferyl alcohol and caffeic acid

The phenolic substrates sinapyl alcohol, coniferyl alcohol or caffeic acid (5 mM) dissolved in 0.5 mL of ethanol (2.5%) and 18.5 mL of 100 mM potassium phosphate buffer (pH 8.0) was added into a 100 mL round-bottom flask. Then 1 mL of CotA laccase (~1 U / mL) was added and the reaction mixture was stirred at 38°C under aerobic conditions. The conversion was followed by thin layer chromatography (TLC) on aluminum sheet Silicagel 60 F_{254} (Merck) using as eluent ethyl acetate + chloroform (3:1) for sinapyl and coniferyl alcohol reactions and methanol + chloroform (1:1) for the caffeic acid reaction. Reactions were performed during 2 h and stopped by addition of 20 mL of methanol. The solvent was evaporated using a Büchi Rotavapor R-205 under 150 mbar and 50°C. After solvent evaporation the products were dried under vacuum for 2 h and the soluble and insoluble fractions were separated by gravity filtration with methanol. The insoluble fraction was dried under vacuum and kept at 4°C whereas the soluble products were evaporated and dried under vacuum for ^1H NMR analysis.

2.12.2 Time-course reactions with CotA-laccase

The phenolic substrates (5 mM) were dissolved in 1 mL of ethanol and added along with 40 mL of phosphate buffer (pH 8.0) into a 100 mL round-bottom flask. Then CotA laccase (~ 1 U / mg substrate) was added and the reaction mixture was stirred at 38°C under aerobic conditions. Reactions were performed during 1 h, where fractions of 10 mL at 15 min, 30 min, 45 min and 60 min of reaction were collected into a 50 mL round-bottom flask and stopped by addition of 10 mL of methanol. The solvent was evaporated and the products were dried under vacuum for 2 h. The soluble and insoluble fractions were separated by gravity filtration with methanol. The insoluble fraction was dried under vacuum and kept at 4°C whereas the soluble products were evaporated and dried under vacuum for ^{1}H NMR analysis.

2.12.3 Reactions with sinapyl alcohol with fast and slow addition of enzyme

Sinapyl alcohol (30 mg, 48 mM) dissolved in 3 mL acetonitrile (0.3 mL, 10%) and 100 mM potassium phosphate buffer (pH 8.0) or 100 mM Britton Robinson buffer (pH 4.0 or pH 10.0) was added into a 100 mL two-neck round bottom flask. For reactions with “fast” addition of enzyme a solution of 50 mL of CotA laccase (0.1 U/ mg substrate) diluted in Britton-Robinson buffer was added and the reaction stirred at 50°C under aerobic conditions for 6 h. For the reactions with slow addition of enzyme, a solution of 50 mL of CotA laccase (0.1 U/ mg substrate) or McoA 15E6-loop5 (0.1 U/ mg substrate) diluted in potassium phosphate or Britton-Robinson buffer was added in a rate of 10 mL / hour and the reaction was stirred at 50°C under aerobic conditionsfor 6 h. The reaction mixture was extracted twice using 50 mL of dichloromethane. The organic fraction was dried with anhydrous sodium sulfate and then transferred into a 100 mL round-bottom flask for solvent evaporation and vacuum drying, while the remaining aqueous solution was extracted twice with 50 mL of ethyl acetate. The organic fraction was dried with anhydrous sodium sulfate and collected for solvent evaporation and product drying. Both residues were analyzed by ^{1}H NMR.

2.13 Proton nuclear magnetic resonance (^{1}H NMR)

^{1}H NMR spectra were recorded on a Bruker Avance (400 MHz) spectrometer in CD_3OD-d^4 $(CD_3)_2CO$-d^6 and DMSO-d^6 as solvents with a 5 mm probe. Spectra were referenced to the residual ^{1}H signal of the deuterated solvent. The following abbreviations are used in reporting the NMR data: s (singlet), d (doublet), t (triplet) and m (multiplet)). Coupling constants (J) are in Hz. Spectra are reported as follows: chemical shift (δ, ppm), multiplicity, integration, coupling constants (Hz).

2.14 Library construction by error-prone PCR (epPCR) using Mutazyme II DNA polymerase

Error-prone PCR using Mutazyme II DNA polymerase (GeneMorph II Random Mutagenesis Kit (Stratagene)) was performed to introduce random mutations in *mcoA* genes. Primers 5′-CATATGTTGAGTAAACAATCCCTCAATATCCCC-3′ (mcoA-182D) and 5′-GACTTGAATTCTCAACATATTGCACC-3′ (mcoA-1816R) were used for amplification (nucleotides for restriction sites of *Nde*I and *Eco*RI are underlined). Each amplification reaction was performed in 50 µL

final volume containing 115 ng of DNA template, 0.25 µM of primers, 800 µM of dNTPs, 2.5 U Mutazyme II DNA polymerase and Mutazyme II polymerase buffer. PCR was performed with initial denaturation period of 2 min at 95°C, followed by 20 cycles of amplification (0.5 min at 95°C, 0.5 min at 55°C and 1.5 min at 72°C), and a final extension step for 10 min at 72°C, executed in a thermal cycler (MyCyclerTM thermocycler, Biorad). The PCR products were digested with *Dpn*I, in order to cleave methylated parental DNA at GATC region at 37°C for 3 h, after which were purified using GFX PCR DNA and Gel Band Purification kit (GE Healthcare) and subjected to electrophoresis in TAE buffer (100 V for 45 min). The final PCR products and plasmid pET-21a(+) Novagen were digested with *Nde*I and *Eco*RI at 37°C for 2 h and pET21a(+) was simultaneously dephosphorylated with 1 U of Alkaline Phosphatase (FastAP, Thermo Scientific) to prevent vector self-ligation. The PCR digested products were cloned into plasmid pET-21A (+) Novagen. These plasmids expressing *mcoA* variants were used to transform electrocompetent *E. coli* Tuner ΔcueO::kan cells.

2.15 "Activity-on-plate" screening

E. coli Tuner ΔcueO::kan cells expressing *mcoA* wild-type or its evolved variants resultant from epPCR, were grown overnight at 37°C on solid LA medium, supplemented with ampicillin (100 µg/L), kanamycin (10 µg/L) and 0.05 mM IPTG. Colonies were transferred onto a chromatography filter paper (Whatman). Master plates were re-incubated for 5 h at 37°C until colonies appeared and afterwards kept at 4°C. The colonies were carefully lysed by soaking the chromatography filter paper in a solution of lysozyme (0.5 µg mL^{-1}) in 20 mM Tris-HCl, pH 7.6 and incubated at 37°C for 2 h. The filter papers were then carefully soaked in a $CuCl_2$ solution (2.5 mM), so proteins could incorporate copper, and incubated at 37°C for 30 min and then soaked in a solution containing 1 mM of substrate 2,6-DMP in 100 mM phosphate buffer, pH 8.0, and incubated overnight at room temperature. The colonies that showed dark orange color were the ones revealing increased enzymatic activity.

2.16 Plasmid extraction

The colonies of variants showing increased activity were picked and grown in a falcon with LB medium at 37°C, at 170 rpm overnight. Cells were harvested by centrifugation (2750*g* at 4°C for 10 min) and plasmids were extracted using GeneJET Plasmid Miniprep Kit (ThermoScientific). Mutations were verified by DNA sequencing analysis using T7 terminator universal primers.

2.17 Expression of *mcoA* variants in *E. coli* in 96-well plates

Colonies of the most active variants were picked from the original transformation plate with a sterile toothpick and transferred to 96-well plates containing 200 µL of LB medium supplemented with ampicillin (100 µg/L) and kanamycin (10 µg/L). Only the central wells were used for cell growth, with exception of B2 and C2 wells used as blank (peripheral wells were filled with water in order to decrease evaporation). Four wells in each plate were used to inoculate the parental strain as controls. Plates were incubated overnight at 37ºC at 750 rpm in a Titramax 1000 shaker (Heidolph). Twenty microliters of each well of the pre-inoculum plates were inoculated in 96-well plates containing 180 µL of TB medium supplemented with ampicillin (100 µg/L) and kanamycin (10 µg/L). Cultures were incubated at 750 rpm,

at 37°C for 4 h, after which *mcoA* gene-expression was induced by adding 0.1 mM IPTG and 0.25 mM $CuCl_2$. Cultures were incubated under the same cultivation conditions during 4 h, after which the shacking was turned off and cells were incubated static overnight.

2.18 Cell disruption and High-throughput activity screening in 96-well plates

The OD_{600nm} was determined in order to calculate Coefficients of Variance (CV = (standard deviation/mean) × 100%) and after that, cells were harvested by centrifugation (2750*g* at 4°C for 10 min). Cells were disrupted by 3 cycles of freeze and thaw by submerging the 96-well plates in liquid nitrogen and then thawed for 5 min at room temperature and then resuspended in 100 μL 20 mM Tris-HCl at pH 7.6 and centrifuged (2750*g* at 4°C for 10 minutes). Supernatants were used for activity measurements. Crude cells extracts (20 μL) were transferred into 96-well plates, and the activity was assayed by adding 180 μL of 100 mM phosphate buffer, pH 8.0 containing 10 mM 2,6-DMP. The reaction was followed at 468 nm on a Synergy 2 (Bioteck) microtiter plate reader

3. Results and Discussion

3.1. Characterization of native and engineered laccases

3.1.1. Cultivation of microorganisms

In order to investigate native and engineered laccases, it was first performed large scale growths of *E. coli* Tuner ΔCueO::kan (DE3) transformed with pET-21a(+) plasmid containing the native laccase *cotA* gene from *Bacillus subtilis*, (pLOM10) (Martins et al., 2002), or the genes coding for the engineered laccases McoA 15E6-loop5 (pMcoA15E6-loop5) and McoA 23B3 (pMcoA23B3). The growths were performed at optimal conditions of temperature, pH and aeration and were monitored during 24 h. The three recombinant strains showed similar growth curves, attaining *log* phase within the first hours of growth and stationary phase after around 6 h (Figure 3.1). The production of proteins of interest was induced by adding IPTG to the medium in the middle of the *log* phase. As *E. coli* Tuner itself is a strain that contains a mutation in the lac permease (lacZY) gene, which permits uniform entry of IPTG throughout the cells of the population, similar levels of protein expression throughout all cells in a culture was achieved. At the same time, copper was also added to the medium and the shaking was stopped 4 h after induction to shift to anaerobic conditions since Durão (2008a) noted that shifting from aerobic to anaerobic (or microaerobic) conditions, cells tend to accumulate higher copper content, which result in the production of copper-full loaded enzymes. Indeed, *E. coli* homeostasis mechanism under aerobic conditions (in contrast to anaerobic) mantains intracellular levels of copper within a narrow range due to the cytotoxic effect of this metal (Madzak et al., 2006), impairing the heterologous production of Cu- fully loaded enzymes. In addition, at the time of IPTG-induction, the temperature was downshifted to 25°C to avoid the accumulation of recombinant proteins in inclusion bodies. The final OD_{600} under microaerobic conditions for *E. coli* cells expressing *cotA*, *mcoA* 15E6-loop5 and *mcoA* 23B3 were 3.4, 3.4 and 2.8, repectively, and whithin the values observed previously (Durão (2008a)).

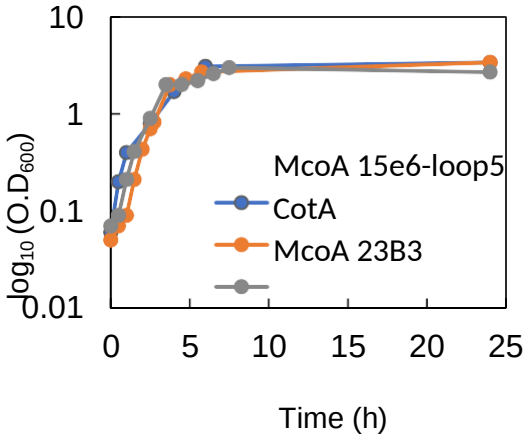

Figure 3.1: Growth of recombinant *E. coli* Tuner ΔCueO::kan (DE3) overproducing wild-type CotA-laccase and McoA 15E6-loop5 and McoA 23B3 engineered laccases. The gene expression was induced at OD_{600}=0.8 with addition of IPTG (1 mM). At this time $CuCl_2$ (2.5 mM) was added and temperature was downshifted from 37 to 25°C. The agitation was stopped 4 h after induction and cells were incubated overnight.

3.1.2. Protein purification

Recombinant CotA, McoA 15E6-loop5 and McoA 23B3, were purified through three purification steps. The first was performed by heating the cell crude extracts at 80°C (CE_{80}) where only thermostable proteins (as it is the case of proteins under study) were not denatured. For maximum enzyme purification fold, the supernatants of heated cell crude extracts were subsequently purified by a two-step protein purification chromatographic procedure.

In figure 3.2a the ion-exchange chromatograms of SP-Sepharose and Q-Sepharose columns, used for purification of CotA-laccase and McoA proteins, respectively are shown. From previous experiments it was already known that CotA and McoA elute around 50% and 30% of buffer B (green line), respectively, that are shown as red dashed rectangles. The presence of CotA-laccase and McoA proteins in those fractions was confirmed by SDS-PAGE (Figure 3.2b) that showed a major band of ~65 kDa for CotA-laccase (Figure 3.2Ab) and two major bands of ~ 55.5 and 35 kDa in the case of McoA proteins (Figures 3.2Bb and 3.2Cb). These two bands were previously identified as McoA, using MALDI-TOF/TOF analysis; it was inferred that the ~ 55.5 kDa form represents the fully denatured form and the faster migrating ~ 35 kDa species most likely represents a partially unfolded form of the enzyme (Brissos et al, 2015). These fractions were concentrated and applied in a Superdex 200 HR 16/60 column for size exclusion chromatography, whose chromatograms are represented in Figures 3.2c. The eluted fractions indicated by the red dashed rectangles showed activity towards a typical laccase substrate, ABTS, and were analyzed by SDS-PAGE (Figures 3.2Ad, 3.2Bd and 3.2Cd).

In order to assess protein purity, samples after the three purification steps (80°C heating, ion exchange and size exclusion chromatographies) were analyzed by SDS-PAGE. It is possible to observe, that all proteins were purified to apparent homogeneity (see McoA 23B3, as example in Figure 3.3).

3.1.3. Spectroscopic characterization

CotA-laccase was produced at higher yields (6.3 mg/L) when compared with McoA 15E6-loop5 and 23B3 (4.4 and 2.8 mg/L, respectively) (Table 3.1). After purification, the enzymes showed the typical blue color. This derives from the copper–cysteine linkage at type 1 copper site which exhibited an intense absorption at approximately 600 nm in UV-Vis spectrum as showed in Figure 3.4. The UV-Vis spectrum also showed a shoulder at approximately 330 nm due to the antiferromagnetically coupling of the T3 binuclear copper site, suggesting the inclusion of the four copper atoms in the three proteins' copper binding sites, since the type 3 coppers are the last incorporated into the protein (Durão, 2008a). Indeed, the BCA quantification assay showed the predictable ratio of ~ 4 mol of copper per mol of protein monomer for CotA and McoA proteins, as indicated in Table 3.1.

Table 3.1: Protein production and copper content of CotA, McoA 15E6-loop5 and McoA 23B3.

Protein	Protein production (mg/L)	Copper content (mol Cu/ mol Protein)
CotA	6.3	4.9
McoA 15E6-loop5	4.4	5.4 ± 0.4
McoA 23B3	2.8	5.3

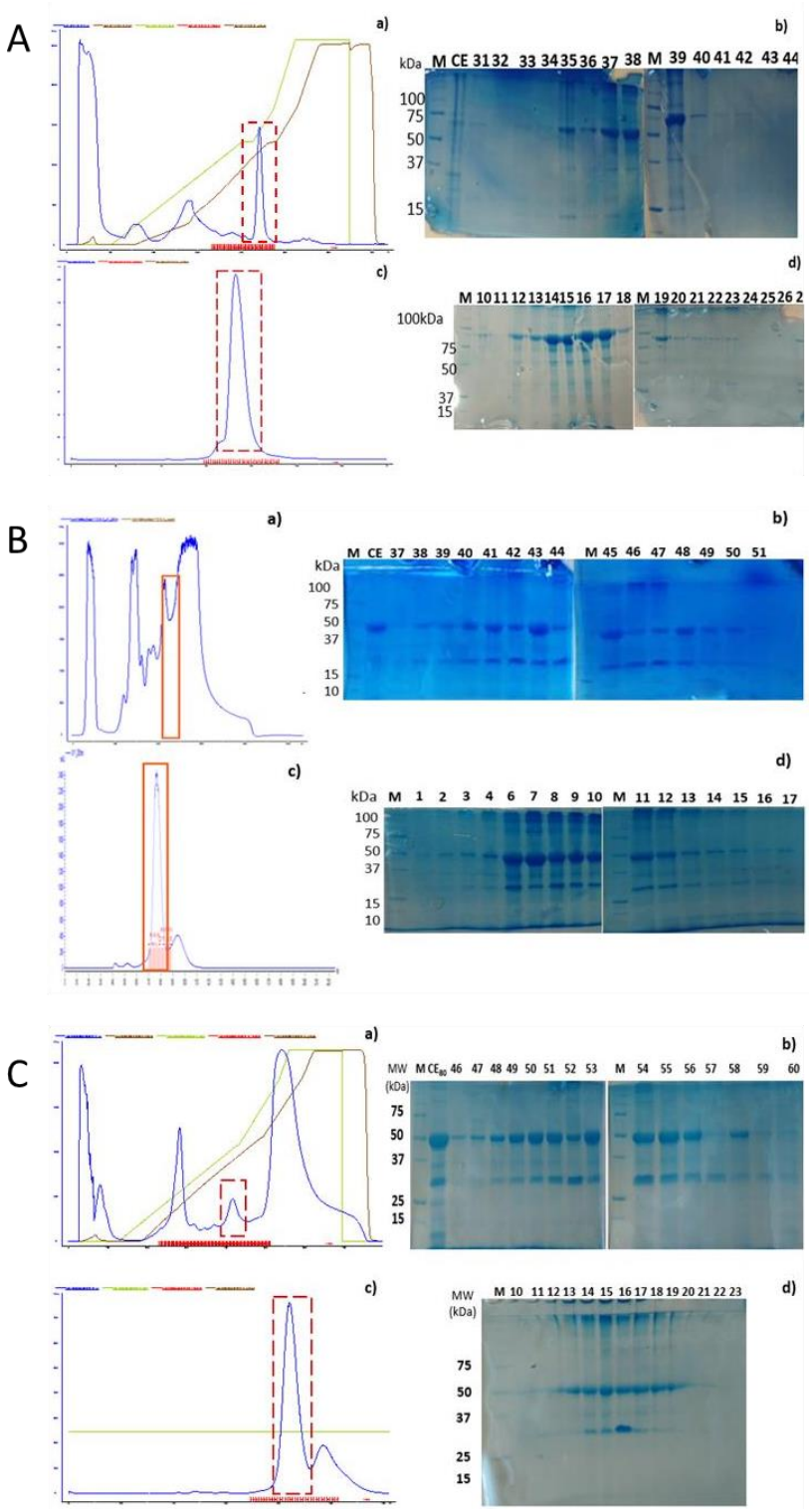

Figure 3.2: Protein purification of **A -** CotA-laccase, **B –** McoA 15E6-loop5 and **C –** McoA 23B3. **a)** Chromatogram of ion exchange chromatography using a SP-Sepharose for CotA-laccase and Q-Sepharose column for McoA 15E6-loop 5 and 23B3 purification. Absorbance at 280 nm (blue line); conductivity (brown line); fractions (red); percentage of Buffer B (green line). Protein of interest (red dashed rectangle); **b)** SDS-PAGE with protein fractions after ion exchange chromatography along with a molecular weight marker (M) and crude extract heated at 80°C (CE/CE_{80}); **c)** Chromatogram of size exclusion chromatography for CotA-laccase and McoA 15E6-loop5 and 23B3 purification using a Superdex 200 HR 16/60 column. Absorbance at 280 nm (blue line); percentage of Buffer B (green line); fractions (red); protein of interest eluted (red dashed rectangle); **d)** SDS-PAGE with protein fractions from size exclusion chromatography along with a molecular weight marker.

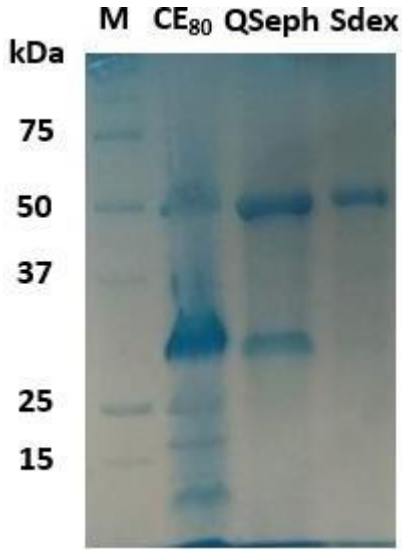

Figure 3.3: SDS-PAGE with samples from all McoA 23B3 purification steps (20 µg of CE_{80} sample, 10 µg of Qseph sample and 2 µg of Spdex sample) and molecular weight markers (M).

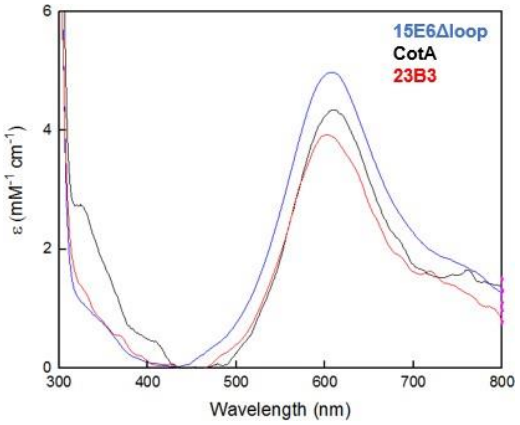

Figure 3.4: UV-Vis spectra of CotA (black line), McoA 15E6-loop5 (blue line), and McoA 23B3 (red line).

3.1.4 Lignin-related phenolics optical characteristics

Thirteen different lignin-related phenolics compounds from the three phenolic-types syringyl, guaiacyl and hydroxyphenyl were used to test the enzymatic activity of the enzymes under study. To calculate the enzymes' specific activities for these compounds one needs to know the substrates' molar extinction coefficient (ε) that most likely vary with pH. The ε values were previously determined for most of the substrates studied, but they were unknown for coniferyl alcohol, vanillin, caffeic acid and *p*- coumaric acid. Thus, the ε values for these substrates, at pH 4.0 and pH 8.0, were determined using the Lambert-Beer law, as described in 2.10 (Table 3.2). The graphs that allowed determining these values for coniferyl alcohol, vanillin, caffeic acid and p-coumaric acid are in the Appendice section (Figure S3).

Table 3.2: Lignin-related phenolics chemical structure, p*K*a, maximal absorption wavelength and molar extinction coefficient (ε) at pH 4.0 and pH 8.0. Phenolics with * had their ε determined experimentally at pH 4.0 and 8.0 during this study.

Lignin-related phenolics	Chemical Structure	p*K*a	λ (nm)	ε (M^{-1} cm^{-1}) at pH 4.0	λ (nm)	ε (M^{-1} cm^{-1}) at pH 8.0
Syringyl-type						
2,6-DMP	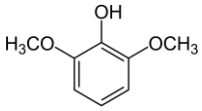	9.98 [a]	468	49,600	468	49,600
Sinapyl Alcohol	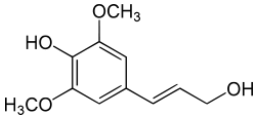	9.4 [b]	275	8,523	275	5,738
Sinapic Acid	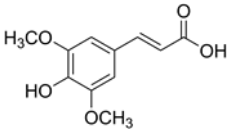	9.2 [a]	310	19,528	310	16,000
Methylsyringate	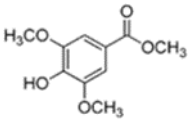	8.7 [a]	275	7,846	320	12,461
Acetosyringone	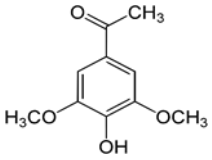	7.88 [a]	300	7,076	360	12,000
Syringaldehyde	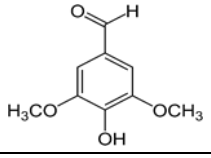	7.34 [a]	300	6,923	360	16,000
Guaiacyl-type						
Coniferyl Alcohol *	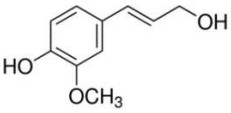	9.54 [a]	265	9,487 ± 192	265	9,697 ± 69
Ferulic Acid	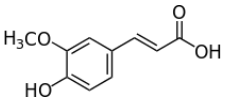	9.39 [a]	310	15,538	310	13,092
Coniferyl Aldehyde	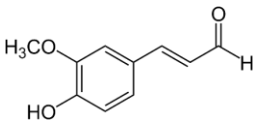	7.94 [a]	350	20,615	350	14,938
Guaiacol	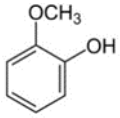	9.93 [a]	470	26,600	470	26,600
Vanillin *	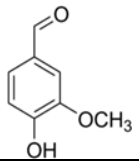	7.4 [a]	310	7,290 ± 133	340	13,835 ± 835
***p*-Hydroxyphenyl-type**						

Caffeic Acid *	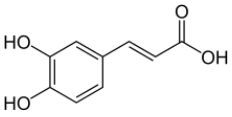	8.6 [c]	320	13,803 ± 625	320	11,744 ± 8
p-Coumaric Acid *	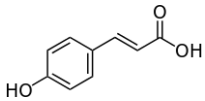	9.92 [d]	290	15,354 ± 410	290	17,560 ± 434

[a] Ragnar, Lindgren & Nilvebrant (2000)
[b] NET - https://foodb.ca/compounds/FDB031178
[c] Genaro-Mattos, Maurício, Rettori, Alonso & Hermes-Lima (2015)
[d] Benvidi et al. (2019)

3.1.5 Comparative pH activity profiles of CotA and engineered laccases analysis

In order to know the optimal pH of the studied enzymes, reactions were performed in the pH range 3 to 12 at room temperature. Substrates tested were the typical non-phenolic laccase substrate ABTS, and the phenolic substrates affiliated to the three phenolic-types, syringyl (2,6-DMP, sinapyl alcohol and sinapic acid), guaiacyl (coniferyl alcohol, coniferyl aldehyde, ferulic acid and guaiacol), and hydroxyphenyl (caffeic acid, *p*-coumaric acid). The optimal pH for CotA laccase was previously shown to be around pH 4 towards ABTS (with a monotonic pH profile) and pH 7.0-9.0 (bell-shape profile) towards some of the phenolics (Brander et al., 2014; Brissos et al., 2012; Reiss et al., 2013; Rosado et al., 2012), while the engineered laccases pH profile needed to be assessed. ABTS pH profiles for both engineered laccases were bell-shaped with maximal at around pH 6 (Figure 3.5), showing an upshift of 2 pH units as compared to the data previously reported for CotA.

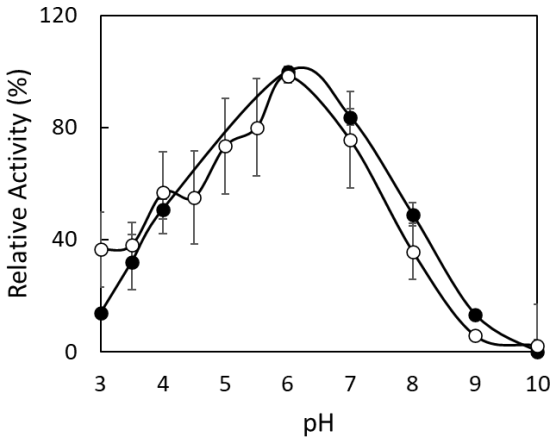

Figure 3.5: pH profiles for ABTS of McoA 15E6-loop5 (filled circles) and McoA 23B3 (open circles).

All studied enzymes showed bell-shaped pH profiles for phenolic compounds with maximal oxidation rates at 7-8, with exception of caffeic acid (pH_{op} ~ 6) (Figure 3.6). Optimal pH for methylsyringate, syringaldehyde and acetosyringone for CotA were previously reported by Rosado et al. (2012) studies, as 9, 8 and 8, respectively.

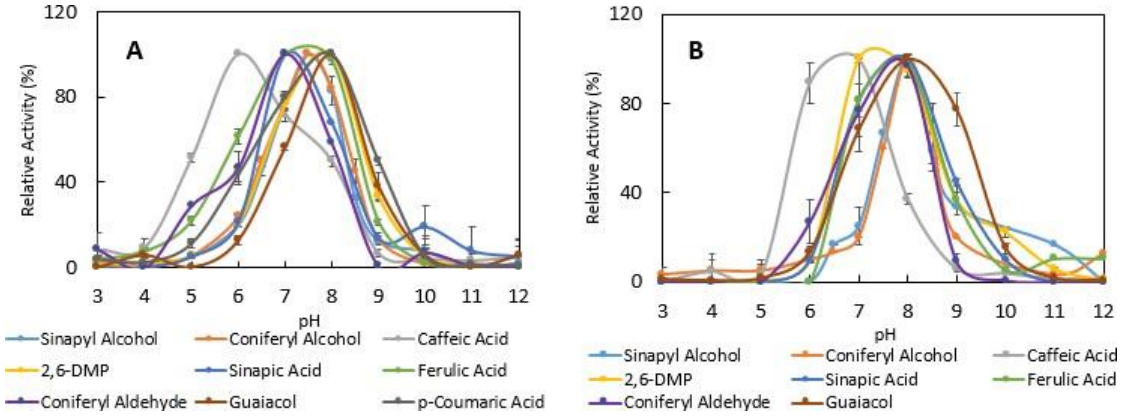

Figure 3.6: pH profiles of CotA-laccase **(A)** and McoA 15E6-loop5 **(B)** for sinapyl alcohol, coniferyl alcohol, caffeic acid, 2,6-DMP, sinapic acid, ferulic acid, coniferyl aldehyde, guaiacol and *p*-coumaric acid. *P*-coumaric acid only had activity towards CotA.

In bacterial laccases, the optimal pH for hydrogen donating substrates (e.g. phenolics) is reported to be within the neutral to alkaline range (Jänhert et al., 2014). The phenolics under study exhibit acid-base transitions with pK_a values ranging from 7.34 to 9.98 (Table 3.2), and it is well known that bacterial laccases, in contrast to fungal laccases, usually attain maximal oxidation rates when the substrates are in the phenolate form, i.e. after deprotonation of their phenolic hydroxyl groups, above pK_a values. Indeed, phenolic compounds, when deprotonated, exhibit lower redox potential and, thus, are more easily oxidized. Intriguinly, the optimum pH for the oxidation of caffeic acid for all tested laccases was under the respective compound's pK_a values, since caffeic acid phenolic hydroxyl group is charged earlier in the pH range (Brander et al., 2014). In contrast to the phenolic compounds, ABTS's optimum pH for most tested laccases is at acidic conditions (Arregui et al., 2019; Brander et al., 2014; Delavari & Perez, 2013; Durão, 2008b; Martins et al., 2015; Reiss et al., 2013; Rosado et al., 2012).

In conclusion, the major observed differences relates to the fact that engineered McoA laccases showed pH optimal for ABTS at 2 units higher than CotA showing an increased alkali-tolerance, while optimal pH for phenolics, around pH 8, are similar in all tested enzymes. Hence, the steady-state kinetics studies for these compounds were performed at this pH value.

3.2 Kinetic parameters comparison between native and engineered laccases

The engineered McoA laccases were evolved through directed evolution to attain higher activity towards 2,6-DMP, having as starting point a variant, 2B3, that was evolved from the parent wild-type enzyme for higher activity for ABTS (Brissos et al., 2015). The catalytic efficiency of engineered McoA laccases for ABTS was found one-order of magnitude lower than that of CotA and 2B3 (24×10^4 M^{-1} s^{-1}, Brissos et al., 2015) (Table 3.3 and Figure 3.7), nevertheless 10-fold higher catalytic efficiency than that of wild-type McoA (33×10^2, Brissos et al., 2015). The relative low efficiencies of McoA enzymes are mainly due to the K_m term, 50 to 70-fold higher than in CotA.

Table 3.3: Kinetic parameters for ABTS of CotA, McoA 15E6-loop5 and McoA 23B3 at optimal pH.

Protein	k_{cat} (s^{-1})	K_m (mM)	k_{cat}/K_m (M^{-1} s^{-1})
CotA	56 ± 2	0.07 ± 0.01	(84 ± 11) × 10^4
McoA 15E6-loop5	284 ± 6	3.6 ± 0.2	(79 ± 5) × 10^3
McoA 23B3	123 ± 19	5 ± 2	(25 ± 10) × 10^3

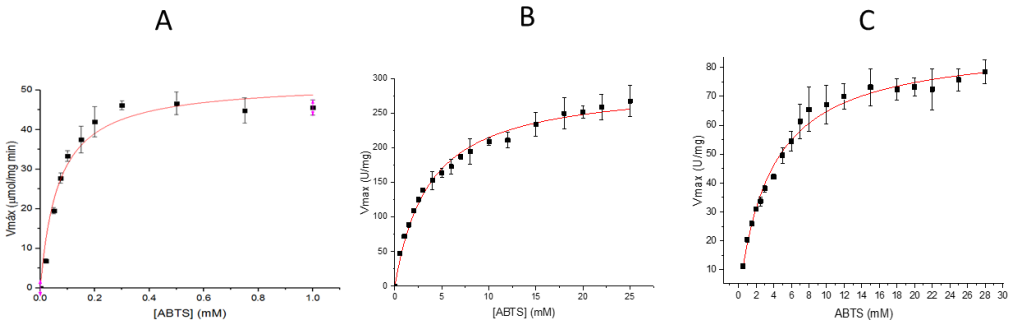

Figure 3.7: Michaelis-Menten kinetics equation by non-linear regression using Origin-Lab software for CotA **(A)**, McoA 15E6-loop5 **(B)** and McoA 23B3 **(C)** towards ABTS (non-linear regression using Origin-Lab software).

The kinetic parameters (k_{cat}, K_m *and* k_{cat}/K_m) of the enzymes CotA, McoA 15E6-loop5 and McoA 23B3 for the phenolic compounds listed in Table 3.4 were determined at room temperature at pH 8, which is the optimal or close to the optimal for most substrates. The data were fitted using Michaelis−Menten equation by non-linear regression and plots for all substrates (Figures S4-S6).

Bacillus subtilis CotA-laccase oxidized all 13 tested phenolics substrates in contrast to the engineered laccases that show no enzymatic activity, in the tested conditions, for 5 of them, syringaldehyde, acetosyringone, methylsyringate, vanillin and *p*-coumaric acid (Table 3.4 and Figure 3.8). Nevertheless, for the remaining 8 substrates oxidized by the three enzymes, the McoA enzymes show catalytic efficiencies similar to those of CotA, especially for the phenolics sinapyl alcohol, 2,6-DMP, coniferyl alcohol and caffeic acid (Table 3.4 and Figure 3.8C). Moreover, the lower catalytic efficiencies observed for McoA enzymes towards some phenolics when compared to CotA, always at the same order of magnitude, are mostly due to the higher K_m values (Table 3.4 and Figure 3.8B) since the k_{cat} values are very similar (Table 3.4 and Figure 3.8A). It was also observed that McoA 23B3 showed no improvement over McoA 15E6-loop5 for phenolics oxidation, as noted previously for 2,6-DMP (Figure 3.8). Therefore, the lineage of evolved McoA proteins should continue from the 15E6-loop5.

The best oxidized substrates affiliated to each of the three phenolic types (syringyl, guaiacyl and hydroxyphenyl) were sinapyl alcohol, coniferyl alcohol and caffeic acid, for the three proteins. The catalytic efficiency for these substrates is in the order of 10^3 - 10^4 $M^{-1}{\cdot}s^{-1}$, accordingly to the higher k_{cat} values of the enzymes (Table 3.4 and Figure 3.8). The k_{cat} (Figure 3.8A) and catalytic efficiencies (Figure 3.8B) values diminished in the following order: sinapyl alcohol > coniferyl alcohol > caffeic acid. In general, it is also possible to observe that within each group of substrates, the order of oxidative rates

decrease as it follows: syringyl > guaiacyl > *p*-hydroxyphenyl phenolics (Table 3.4 and Figure 3.8), indicating that the phenolic type have a preponderant role in the enzymes' oxidative rate. This is probably due to the fact that laccases' oxidative rates are influenced by substituents at *ortho* positions, as reported by several studies (Mehra et al., 2018; Pardo & Camarero, 2015; Reiss et al., 2011; Xie et al., 2015). In most cases, phenolics *ortho* positions to the OH phenol group are occupied by hydroxyl or methoxy groups with a lone pair of electrons adjacent to the phenol. These substituents, apart from lowering the electrochemical potential of the substrate favoring bacterial laccases' oxidation, have a positive mesomeric effect, enhancing the electron density at the phenoxy-OH, thus facilitating electron abstraction. Previous studies reported that substrates with methoxy groups were preferently oxidized when compared with substrates with hydroxyl groups even though these activate more the aromatic ring. Thus, the order syringyl > guaiacyl > *p*-hydroxyphenyl is in line with the number of *o*-methoxy groups, since syringyl type phenolics are dimethoxylated, guaiacyl type phenolics are monomethoxylated and hydroxyphenyl type phenolics are non-methoxylated. Additionally, *p*-coumaric acid is the only substrate, from the ones tested, without any *ortho* groups of phenolic OH and is, together with vanillin, the substatre for which CotA shows the lowest catalytic efficiency ($24 \pm 1\ M^{-1} \cdot s^{-1}$) and McoA enzymes show no enzymatic activity under the conditions tested. Xie et al. (2015) showed CotA-crystal structure docked with sinapic acid where the two methoxy substituents are at a distance $\leq$ 3Å of the CotA's T1 Cu His419 ligand. Xie et al. (2015) also had observed bonds between sinapic acid and three water molecules and two of them form hydrogen bonds with Arg416, near T1 Cu site of CotA-laccase, leading to a binding stabilization enhancement and a high selectivity of the protein towards the phenolic. Nonetheless, it was observed that deprotonated phenolics' *ortho* OH groups also form bonds with the enzyme, whereas phenolics with no hydroxyl group in the *ortho* positions of phenolic OH showed no hydrogen bond (Mehra et al., 2018). Therefore, bacterial laccases' oxidative rates are indeed dependable of the redox potential threshold, however the substrate docking to the T1 copper site of the protein is a putative important feature for higher catalytic efficiencies, and hence considered the limiting step for laccases' oxidative rates.

The *para*-substituents of phenolic substrates such as carboxyl (*p*-coumaric acid, ferulic acid, sinapic acid and caffeic acid) ketone (acetosyringone), aldehyde (syringaldehyde, coniferyl aldehyde and vanillin), ether (methylsyringate) or alcohol (coniferyl alcohol and sinapyl alcohol) are also important structural features for laccases' enzymatic activity since the presence of α-carbonyl groups, due to their electron-withdrawing nature can lead to reducing oxidative rates. However, the electron-withdrawing effects can be diminished by the presence of double bonds in the side-chain, which stabilizes the forming radical by electron delocalization of the unpaired electrons (Smirnov et al., 2001) or when the carbon-side chain is elongated (Ragnar et al., 2000). The fact that vanillin is the substrate for which CotA shows the lowest catalytic efficiency ($183\ M^{-1} \cdot s^{-1}$) and McoA enzymes show no enzymatic activity under the conditions tested probably relates to the presence of a α-carbonyl group without any double bond in the *para*-postion. Koschorreck et al. (2008) reported that *Bacillus licheniformis* CotA did not presented activity towards vanillin relatives since these molecules are too small for efficient binding. In the absence of *para* substituents, there is a decrease of electronic density on the phenolic hydroxyl oxygen, leading to a more difficult electron abstraction by the enzyme (Kajiyama & Ohkatsu, 2001). The size of the *para*

side chain is also an important factor since the carbon chain affects the hydrophobic effects, resulting in a different mode of binding and orientation of the substrate affecting catalysis. Ragnar (2000) concluded that the elongation of a carbon chain generally decreases the overall pK_a value of the phenolic thus facilitating the oxidation at lower pH values. Indeed, both engineered laccases showed no activity towards all tested substrates with small *para*-side chains such as syringaldehyde, acetosyringone, methylsyringate and vanillin.

Overall, sinapyl alcohol, coniferyl alcohol and caffeic acid, affiliated to each of the three phenolic types, demonstrate the importance of both ortho and para substituents in the achievement of higher oxidation rates. Sinapyl alcohol is dimethoxylated, coniferyl alcohol is monomethoxylated and, caffeic acid is non-methoxylated. Moreover, these substrates have the longest *para* side chains and caffeic acid, while having an α-carbonyl group, has a double bond that potentially stabilizes the radical and attenuates the electron-withdrawing effect.

Table 3.4: Kinetic parameters (k_{cat}, K_m and k_{cat}/K_m) of CotA, McoA 15E6-loop5 and McoA 23B3 for all studied lignin related phenolic compounds at pH 8.0.

	CotA			*McoA 15E6-loop5*			*McoA 23B3*		
Lignin related phenolics	k_{cat} (s^{-1})	K_m (mM^{-1})	k_{cat}/K_m ($M^{-1}\ s^{-1}$)	k_{cat} (s^{-1})	K_m (mM^{-1})	k_{cat}/Km ($M^{-1}\ s^{-1}$)	k_{cat} (s^{-1})	K_m (mM^{-1})	k_{cat}/K_m ($M^{-1}\ s^{-1}$)
Syringy-type									
Sinapyl Alcohol	14 ± 0.1	0.03 ± 0	(49.3 ± 0.3) × 10^4	57 ± 7	0.25 ± 0.05	(23 ± 5) × 10^4	21 ± 3	0.25 ± 0.05	(85 ± 23) × 10^3
2,6-DMP	2.1 ± 0.1	0.1 ± 0.03	(16 ± 4)×10^3	7.6 ± 0.3	0.4 ± 0.07	(19 ± 3) ×10^3	2.9 ± 0.1	0.5 ± 0.1	(59 ± 17) × 10^2
Sinapic Acid	6.0 ± 0.4	0.1 ± 0.01	(70 ± 11) × 10^3	4.6 ± 0.1	0.5 ± 0.04	(94 ± 8) × 10^2	6 ± 1	0.5 ± 0.1	(13 ± 3) × 10^3
Syringaldehyde	1.4 ± 0.2	0.2 ± 0.03	(72 ± 15) × 10^2	n.d.	n.d.	n.d.	n.d.	n.d.	n.d.
Acetosyringone	0.8 ± 0.2	0.1 ± 0.09	(51 ± 33) × 10^2	n.d.	n.d.	n.d.	n.d.	n.d.	n.d.
Methylsyringate	0.3 ± 0.01	0.4 ± 0.2	(71 ± 30) × 10^2	n.d.	n.d.	n.d.	n.d.	n.d.	n.d.
Guaiacyl-type									
Coniferyl Alcohol	6.6 ± 0.3	0.06 ± 0.01	(12 ± 1) × 10^4	17 ± 4	0.23 ± 0.06	(72 ± 27) × 10^3	3.0 ± 0.1	0.2 ± 0.003	(13 ± 1) × 10^3
Ferrulic Acid	3.6 ± 0.3	0.11 ± 0.002	(33 ± 3) × 10^3	1.7 ± 0.3	0.4 ± 0.07	(45 ± 12) × 10^2	0.9 ± 0.1	0.41 ± 0.04	(21 ± 3) × 10^2
Coniferyl Aldehyde	0.9 ± 0.1	0.2 ± 0.04	(45 ± 10) × 10^2	0.2 ± 0.05	0.8 ± 0.3	(20 ± 10) × 10^1	0.1 ± 0.03	0.6 ± 0.3	(21 ± 11) × 10^1
Guaiacol	0.7 ± 0.1	0.7 ± 0.1	(94 ± 21) × 10^1	0.13 ± 0.02	1.6 ± 0.3	(78 ± 17) × 10^0	0.4 ± 0.1	27.4 ± 3.0	(16 ± 4) × 10^0
Vanillin	0.013	0.07	18.3 × 10^1	n.d.	n.d.	n.d.	n.d.	n.d.	n.d.
Hydroxyphenyl-type									
Caffeic Acid	5 ± 1	0.05 ± 0.02	(95 ± 3) × 10^3	7 ± 2	0.19 ± 0.06	(36 ± 16) × 10^3	2.2 ± 0.6	0.1 ± 0.03	(22 ± 9) × 10^3
p-Coumaric Acid	0.021 ± 0.0004	0.88 ± 0.03	(24 ± 1) × 10^0	n.d.	n.d.	n.d.	n.d.	n.d.	n.d.

n.d. – Not detected

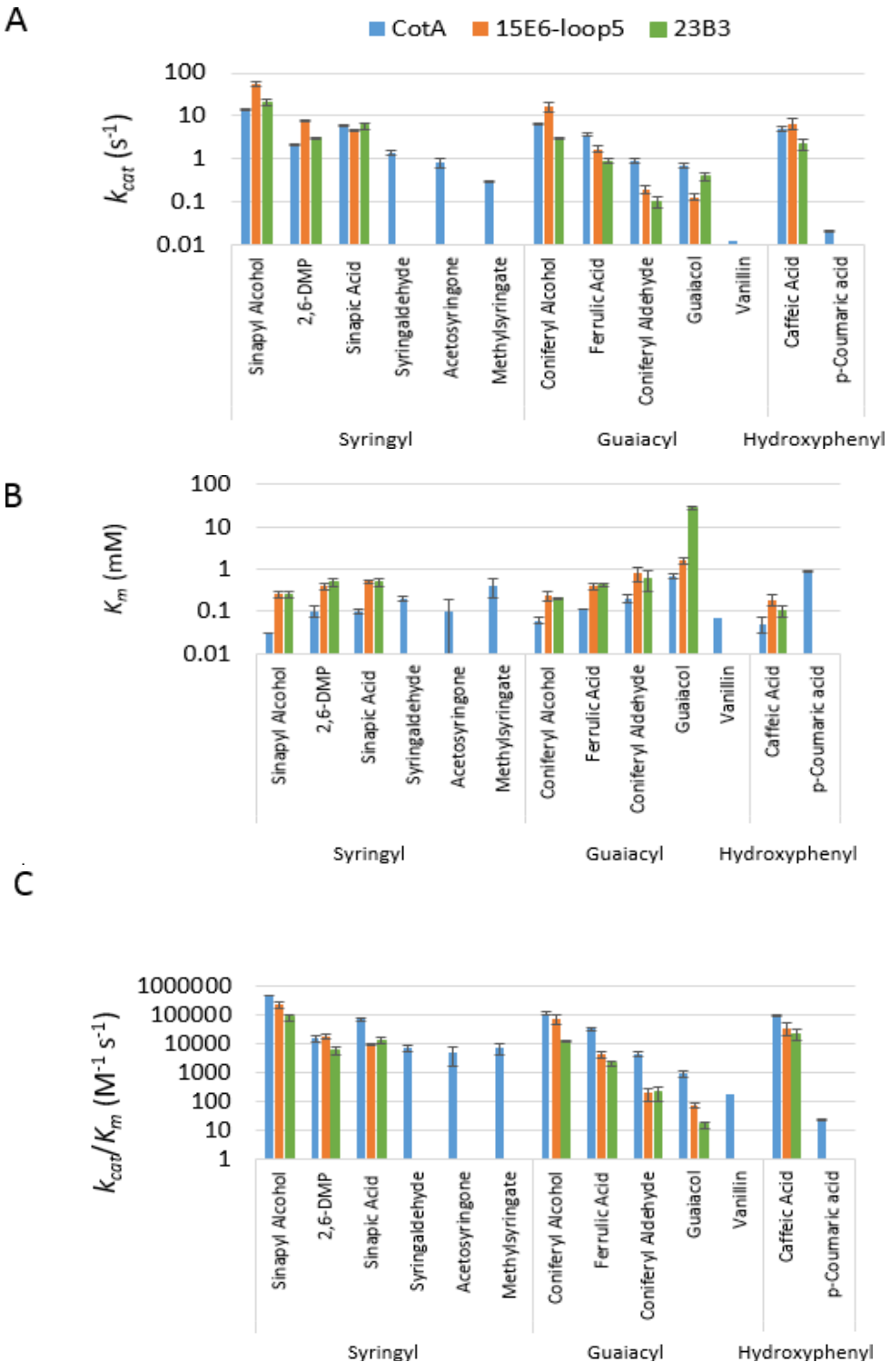

Figure 3.8: Bar chart of k_{cat} (s^{-1}) **(A)** K_m (mM) **(B)** and k_{cat}/K_m (M^{-1} s^{-1}) **(C)** values for CotA (blue), McoA 15E6-loop5 (orange) and McoA 23B3 (green) towards sinapyl alcohol, 2,6-DMP, sinapic acid, syringaldehyde, acetosyringone, methylsyringate, coniferyl alcohol, ferulic acid, coniferyl aldehyde, guaiacol, vanillin, caffeic acid and *p*-coumaric acid.

3.3 Scale-up reactions and identification of products by ^{1}H NMR

The results obtained in the previous experiments showed that the best substrates for both native and engineered laccases were sinapyl alcohol, coniferyl alcohol and caffeic acid. Interestingly, it is reported in the literature that the enzymatic oxidative dimerization of these monolignols can yield syringaresinol (Jaufurally et al., 2016), pinoresinol (Wan et al., 2007) and phellinsin A (Nemadziva et al., 2018), respectively, which are products with medical value. So far, there are no studies reporting synthesis of this products using bacterial laccases. Therefore, time course scale-up reactions of CotA and McoA 15E6-loop5 using these phenolic compounds as substrate were performed and the products were identified using ^{1}H NMR.

First, the scale-up enzymatic reactions were performed using the native laccase (~ 1 U/mg of substrate) towards the substrates sinapyl alcohol (SA1) (Table 3.5), coniferyl alcohol and caffeic acid (5 mM) at pH 8.0, 37°C for 2 h. The ^{1}H NMR spectra of reaction products in CD_3OD showed the total absence of sinapyl alcohol and caffeic acid substrates, whereas the reaction with coniferyl alcohol after two hours still exhibited a small quantity of the starting material, indicating that this enzymatic reaction was incomplete (data not shown). Analysis of the soluble fraction of the reactions showed the presence of low amounts of a complex mixture of products hampering their identification. Furthermore, the existence of insoluble residues indicated that the potential oligomerization of phenoxy radicals formed into several oligomeric and polymeric forms. Therefore, to better analysis of the reactions, a time course analysis was performed for reactions with sinapyl alcohol (SA2) and caffeic acid and aliquots were collected after 15, 30, 45 and 60 min, extracted and then analyzed by ^{1}H NMR. For this set of experiments, coniferyl alcohol was excluded since after 2 h of reaction the presence of substrate was still observed.

^{1}H NMR analysis of the time-course reaction with sinapyl alcohol showed total substrate consumption after 15 min and after 30 minutes, a small amount of a desired product syringaresinol was detected (^{1}H-NMR (CD_3OD, 400 MHz): δ 6.72 (2H,s, H-2 and H-6), 4.72 (1H,d,J 4.6 Hz, H-7, H-7'), 3.14 (1H,m, H-8, H-8'), 3.91 (1 H,m, H-9a, H-9'a), 4.28 (1H,m,H-9b), 6.65 (2H,s, H-2', H-6'), 4.28 (1 H,m, H-9'b), 3.86 (6H,s, 2-OCH_3), 3.84 (6H,s, 2-OCH_3) (Figure 3.9B). However, the signals that corresponded to syringaresinol are not present in spectra after 45 and 60 min of reaction (Table 3.5 and Figure 3.9C). Analysis of reactions with caffeic acid showed that the reaction was slower than with sinapyl alcohol, since the complete absence of substrate was only attained after 60 min (data not shown). A mixture of products is present and no changes in their composition was observed up to 60 min. The presence of several putative products including blechnic acid, 5-5'-caffeic acid, 8,8´-dicaffeic acid, 8,5´-dicaffeic acid, 8,8'-dicaffeic acid aryltetralin, dimer 5-O-4' caffeic was searched in accordance to data in the literature but no matches were found. For these reasons, further reactions were only performed with sinapyl alcohol.

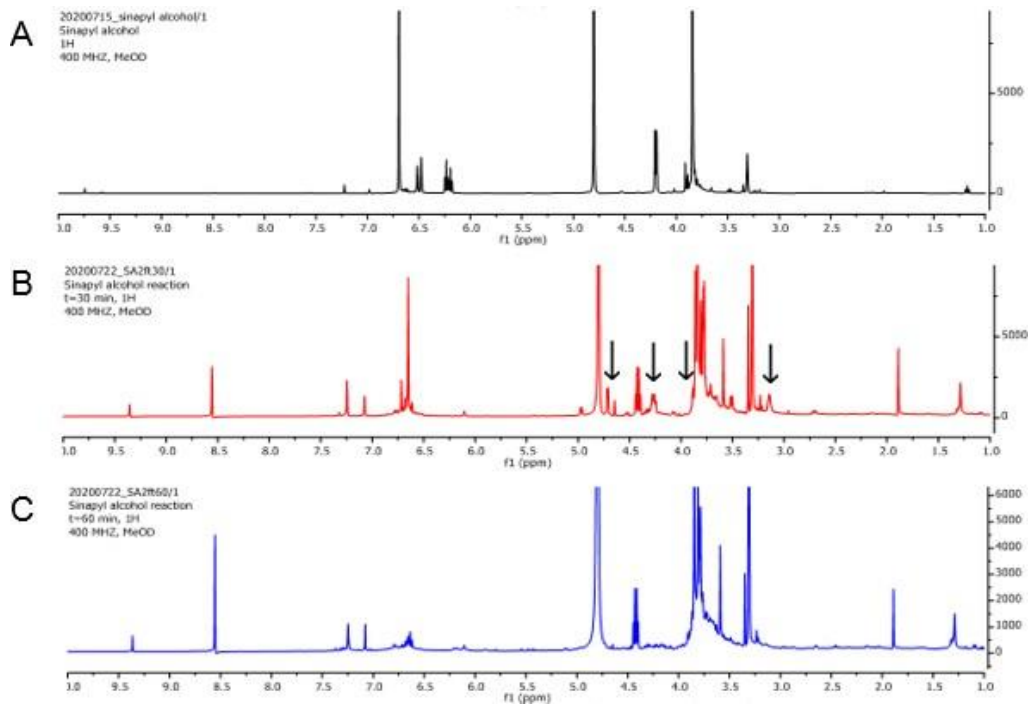

Figure 3.9: Comparison between the ^{1}H NMR spectra in deuterated methanol of the substrate (sinapyl alcohol) (A), the reaction products using CotA laccase after 30 min of reaction with arrows pointing towards syringaresinol signals (B) and at 60 min of reaction (C).

In order to achieve higher yields of syringaresinol from sinapyl alcohol several operating conditions were further optimized based in the report from Jaufurally et al. (2016). These authors used a fungal laccase for the conversion of sinapyl alcohol into syringaresinol and noticed that the mode of addition of the enzyme was an important parameter affecting the yields of the dimer formation. In reactions with slower addition of the enzymatic solution, with a flow of 9 mL/h during 5.5 h, syringaresinol was the major dimer obtained, in contrast with the reactions where all the enzyme was added at the beginning of the reaction which seemed to favor the formation of oligomers. At temperatures from 40 to 50°C with a slow enzyme addition, β-β dimers (syringaresinol) were predominantly obtained, while at lower temperatures, with the same flow of enzyme addition, a mixture of dimers β-β and β-*O*-4 as well as of higher oligomers were obtained. The increase of the substrate:enzyme (Sub:Enz) ratio leading to a reduced the oxidative power of the enzyme, thus controlling the polymerization degree, contributed positively for the synthesis of syringaresinol. The co-solvent was also reported as a relevant parameter for laccase-mediated reactions; using acetonitrile as co-solvent instead of ethanol was proved to be more suitable for laccase-mediated reactions (Jaufurally et al., 2016; Reano et al., 2016). The different yields in syringaresinol production is based on the fact that sinapyl alcohol, upon oxidation, due to its two methoxy groups on the aromatic ring in the ortho positions of the OH phenol group, only has two possible linkages: β-β or β-*O*-4. The β-β bonding, which results from a лл stacking interaction between a sinapyl alcohol phenoxy radical and a non-oxidized sinapyl alcohol molecule,

leads to syringaresinol, while β-*O*-4 linkage, originated by л-л stacking interactions between two phenoxy radicals leads to the formation of β-*O*-4 dimer and higher oligomers. Therefore, the experimental conditions for bioconversion of sinapyl alcohol into syringaresinol have to promote the coupling between radicals and non-oxidized sinapyl alcohol and avoid the incorporation of syringaresinol obtained as substructure in a β-*O*-4 conformation leading to higher oligomers.

Taking into consideration the results reported by Jaufurally et al. (2016), we have set-up a number of experiments (SA3-SA6) changing the pH and temperature of reaction, solvent and the amount and modes of enzyme addition (Table 3.5).

Table 3.5: Summary table of the experimental conditions for reactions with sinapyl alcohol and the results obtained in accordance with the condition. The dark color of the reaction mixture indicates the presence of dimers along with other oligomerization products.

Reaction	pH	Volume$_f$ (mL)	$[SA]_{initial}$ (mM)	$[Enzyme]_{final}$ (U/ mg of substrate)	Buffer	T (°C)	Reaction time (h); Enz addition mode	Workout	Results
SA1	8	20	5	0.95	Phosphate (100 mM) 10% ethanol	37	2; Fast	20mL MeOH, Dry, MeOH extraction	Brown; Mixture of products
SA2	8	40	5	0.95	Phosphate (100 mM) 10% ethanol	37	1; fast	10 mL MeOH, Dry, MeOH extraction	Brown; Mixture of products
SA3	8	53	47.6	0.1	Phosphate (100 mM) 10% acetonitrile	50	5 + 1; slow	DCM extraction + ethyl acetate extraction	Purple after 3h; Mixture of products
SA4	10	53	47.6	0.1	BR buffer 10% acetonitrile	50	5 +1; slow	DCM extraction + ethyl acetate extraction	Bright yellow; Syringaresinol
SA5	10	53	47.6	0.1	BR buffer 10% acetonitrile	50	1; fast	DCM extraction + ethyl acetate extraction	Orange; Syringaresinol and other products
SA6	4	53	47.6	0.1	BR buffer 10% acetonitrile	50	5 + 1; slow	DCM extraction + ethyl acetate extraction	Incomplete reaction; Syringaresinol and sinapyl aldehyde

The new reaction at pH 8 (SA3), where the enzyme was diluted into 50 mL of the buffer solution and was added at a flow of 10 mL/h (slow addition), for a total of 5 h with an extra hour of reaction to assure complete consumption of the substrate, did not showed significant differences in terms of syringaresinol production as compared to the reaction SA2, where the enzyme was added at the starting of the reaction as assessed by ^{1}H NMR spectra (Figure 3.10). We have decided to perform a reaction at pH 10 (SA4) to (i)

decrease the rate of reaction (Figure 3.6) and (ii) to provide conditions where the substrate is deprotonated (pK_a of 9.4 (see Table 3.2)), and, thus, facilitate its oxidation. The analysis of reaction products by ^{1}H NMR spectra (Figure 3.11 or 3.12) showed that under these conditions, the major product of reaction was, the desired product, syringaresinol, with a yield of 66%.

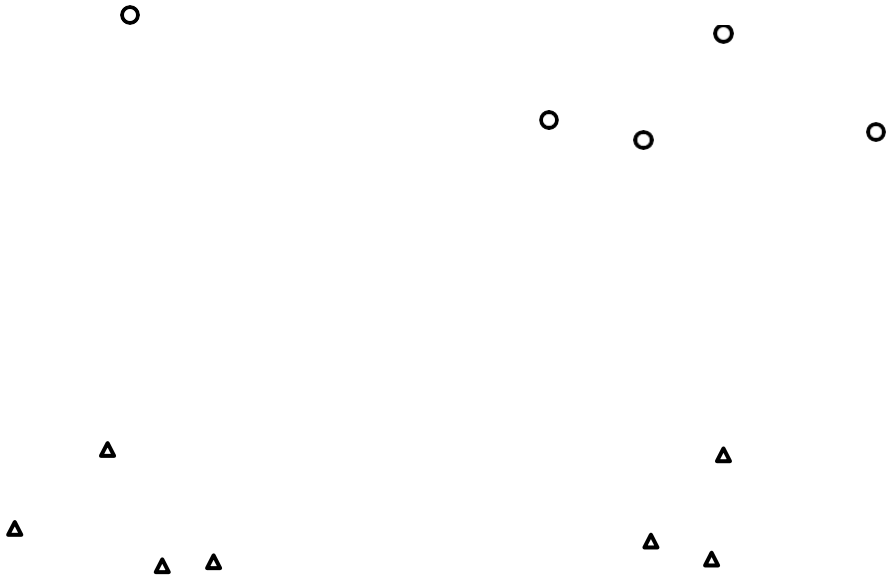

Figure 3.10: ^{1}H NMR spectra of reactions at pH 8 (SA3) and pH 10 (SA4), where the enzyme was added slowly to the reaction mixtures, in deuterated chloroform (open circles, syringaresiol and open triangle sinapyl alcohol). Solvent signals were suppressed for clarity.

In order to understand, which is the most relevant factor for the dimer synthesis, the mode of enzyme addition and/or the protonation state of the substrate, two additional reactions were performed. One at the same conditions of SA4, at pH 10, but with immediate (fast) addition of the enzyme to the reaction (SA5), and one other where the addition of enzyme was slow but the pH was changed to 4 (SA6). This pH value was chosen, because the enzyme at pH 4 and 10 presents similar low catalytic efficiencies towards sinapyl alcohol (Figure 3.6A), but the substrate will be at the protonated form. This reaction was also performed to assess if syringaresinol yields relates to high or low enzymatic activity. The ^{1}H NMR spectra for SA5 as well as for SA6 reaction (Figure 3.11), showed that syringaresinol was obtained, however not as the only product. Both ^{1}H NMR spectra showed the signals for syringaresinol and other impurities like sinapyl aldehyde, meaning that both reactions were not clean. At pH 4, the reaction was incomplete since there were still signals of the starting material, sinapyl alcohol.

As the conditions for solo synthesis of syringaresinol were optimized for the CotA-laccase, a reaction under those same conditions was performed using the variant 15E6-loop5 (SA7). By analysis of the ^{1}H NMR spectra (Figure 3.12), the reaction using the McoA variant was complete and the presence of

syringaresinol was observed although with a lower quantity than the observed using CotA and moreover, it is not the only product of reaction. The yield of the reaction using McoA 15E6-loop5 as biocatalyst was not possible to calculate due to technical issues.

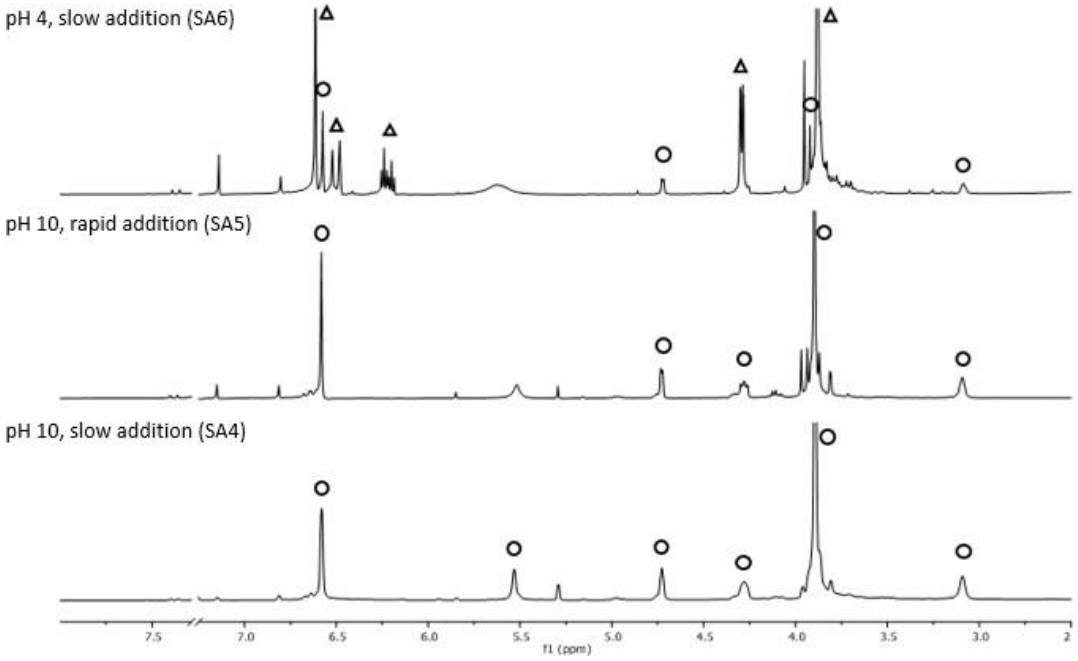

Figure 3.11: ^{1}H NMR spectra of reactions SA4, SA5 and SA6 in deuterated chloroform (open circles, syringaresiol and open triangle sinapyl alcohol). Solvent signals were suppressed for clarity.

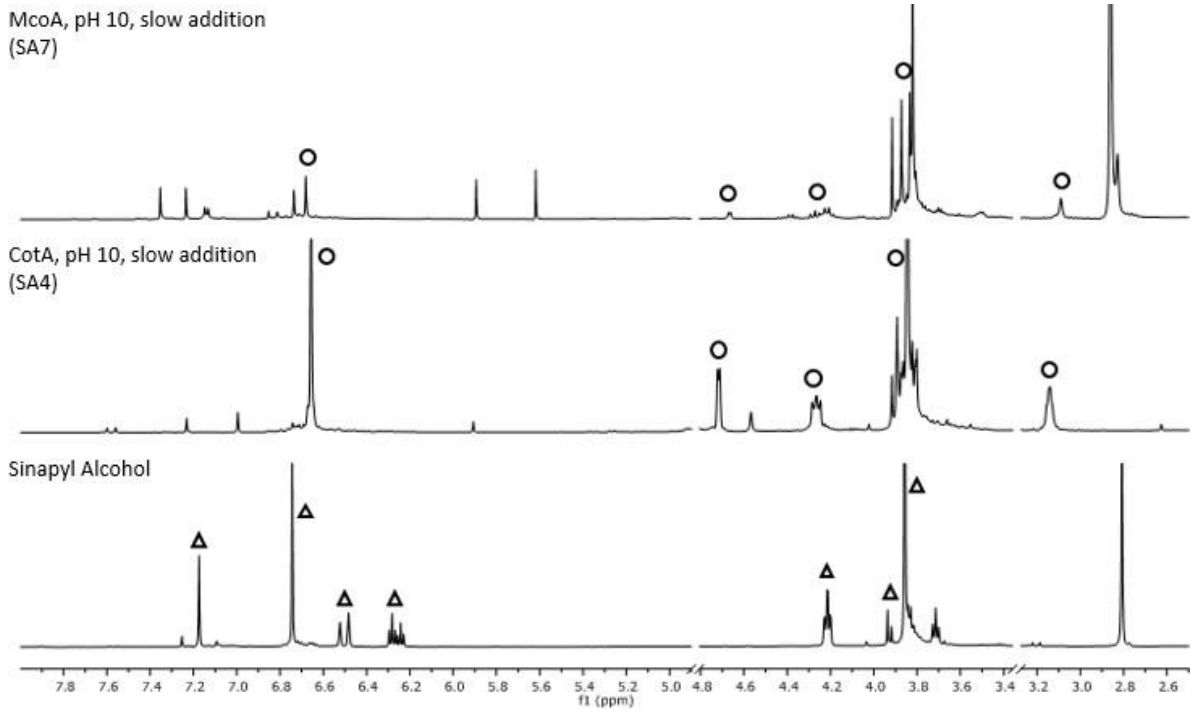

Figure 3.12: ^{1}H NMR spectra of reactions SA7 (using McoA 15E6-loop5) in deuterated acetone, SA4 in deuterated chloroform (using CotA) and the substrate sinapyl alcohol in deuterated chloroform (open circles, syringaresiol and open triangle, sinapyl alcohol). Solvent signals were suppressed for clarity.

The reactions SA1, SA2 and SA3 showed the presence of a mixture of oligomers and while for the $SA2t_{30}$ sample, the signals of syringaresinol were detected, they disappeared shortly after, probably involved in further couplings with other radical species present in the reaction. From the different experimental conditions tested for the enzymatic oxidation of sinapyl alcohol it was concluded that the increase of temperature as well as the substrate:enzyme ratio are not crucial factors for the reaction selectivity towards syringaresinol. On the contrary, the decrease of the enzymatic oxidative rate through pH change (4 or 10) and conditions that promotes the deprotonation of the monolignol (pH 10) demonstrated to be key factors for the syringaresinol synthesis. Both conditions were needed for enhancing the yield of reaction as demonstrated by comparison of the results obtained for the reactions SA4 and SA6. The rate of addition (slow *vs* fast) of the enzyme solution does not seem to substantially affect the course of reaction and the type of products obtained. CotA-laccase oxidation of sinapyl alcohol presented a higher yield of syringaresinol as well as a higher selectivity in comparison with the McoA 15E6-loop5 variant under the same conditions, meaning that the engineered laccase, accordingly to these results, is not as yet as suitable as CotA for industrial applications, and more rounds of evolution are needed to improve McoA kinetic properties.

The reactions for bioconversion of coniferyl alcohol and caffeic acid to pinoresinol and phellinsin A, respectively, require optimization. The oxidation of coniferyl alcohol using CotA resulted in an incomplete and unselective reaction, while caffeic acid's reaction products were insoluble. As future work, coniferyl alcohol reaction could be carried out in higher temperatures for increasing the solubility of the substrate, in a more extensive period of time for complete depletion of the substrate and with a diluted enzyme solution to reduce the oxidative power of the enzyme, thus benefiting the selectivity of the reaction. Whereas the caffeic acid reaction could be executed under the same conditions here reported for sinapyl alcohol that yielded syringaresinol, however with an ideal co-solvent for enhancing the solubility of the substrate and oligomers formed.

There are other lignin-related phenolic compounds here reported whose dimerization can yield added-value lignans, in particular, sinapic acid as source of tyrosol sinapate which is a semisynthetic analogue of (-) oleocanthal that shows several biological effects including anticancer activity (Sun et al, 2018) and and ferulic acid as a source of tanegool that shows diverse pharmacological activity, including a great potential in the prevention of Alzheimer's disease (Carunchio et al., 2001; Sun et al., 2018). As such, should be interesting, as future work, to optimize the conditions for the bioconversion of these phenolics.

3.4 Engineering McoA 15E6-loop5 towards improved activity for lignin-phenolic substrates

All McoA generations for the evolution of McoA were performed using epPCR using the Taq DNA polymerase however, it is known that one of the causes of the mutational bias by epPCR is due to the DNA polymerases. There are several ways to assess bias in an enzyme's mutational spectrum. Bias can be examined by analyzing the ratio of transition (Ts) to transversion (Tv) mutations produced. Transition

mutations are purine (A and G) to purine changes and pyrimidine (C and T) to pyrimidine changes, while transversions are purine to pyrimidine and pyrimidine to purine changes. There are eight possible transversions and four possible transitions, and an enzyme completely lacking bias would exhibit a Ts/Tv ratio of 0.5. Secondly, mutational bias has been assessed by calculating the ratio of AT→GC to GC→AT transition mutations (AT→GC/GC→AT ratio), which would equal 1 for a completely unbiased enzyme. Thirdly, mutational bias can be assessed by comparing the frequency of mutating A's and T's vs. the frequency of mutating G's and C's (AT→NN/GC→NN ratio), which should be equal for an unbiased DNA polymerase. In this work a library of McoA variants was constructed, upon McoA 15E6-loop5, by epPCR using Mutazyme II DNA polymerase, described to produce a less biased mutational spectrum with equivalent mutation rates at A's and T's vs. G's and C's.

First, the PCR conditions were optimized in order to achieve a mutational rate around 1-3 amino acid changes (1-5 nucleotide substitution/gene), by adjusting the initial target DNA amounts in the amplification reactions. For the same PCR yield, targets amplified from low amounts of target DNA undergo more duplications than targets amplified from high concentrations of DNA. The more times a target is replicated, the more errors accumulate. Therefore, lower PCR mutation frequencies can be achieved by using higher DNA template concentrations to limit the number of target duplications. The DNA sequence information of variants showed that the mutation rate was around 1-4 amino acid changes, as intended.

Then, the mutational spectra of this library was compared with the results previously obtained with Taq DNA polymerase. It is important to mention that the analysis was performed with 32 mutations acquired during the laboratory evolution previously performed with Taq DNA polymerase while in the case of Mutazyme II we only have 7 mutations obtained during this study. Generally, epPCR mutational spectra favors transitions over transversions, however in the case of McoA evolution this is much more pronouns in the case of Taq DNA polymerase when compared to the results obtained using Mutazyme II (Table 3.6 and Figure 3.13). Moreover, Taq under error-prone conditions is 7 times more likely to mutate A's and T's than G's and C's, while Mutazyme II DNA is nearly 5 times more likely to mutate G's and C's (Table 3.6 and Figure 3.13). From our results in McoA evolution the DNA polymerases are more bias than what is described in literature and the Mutazyme II does not show equivalent mutation rates at A's and T's vs. G's and C's as described. However, in this specific case, it seems that these two DNA polymerases can complement each other, and it seems worthy to construct a new library using the Mutazyme II tocover mutations that were not introduced using the Taq polymerase.

Table 3.6: Mutational spectra of Taq DNA polymerase and Mutazyme II DNA polymerase.

	Taq DNA		Mutazyme II DNA	
	Literature	McoA evolution (32 mutations)	Literature	McoA evolution (7 mutations)
Ts/Tv	0.8	7	0.9	1.3
AT->GC/GC->AT	1.9	6	0.6	0.2
AT->N/GC->N	3.9	7	1.2	0.2

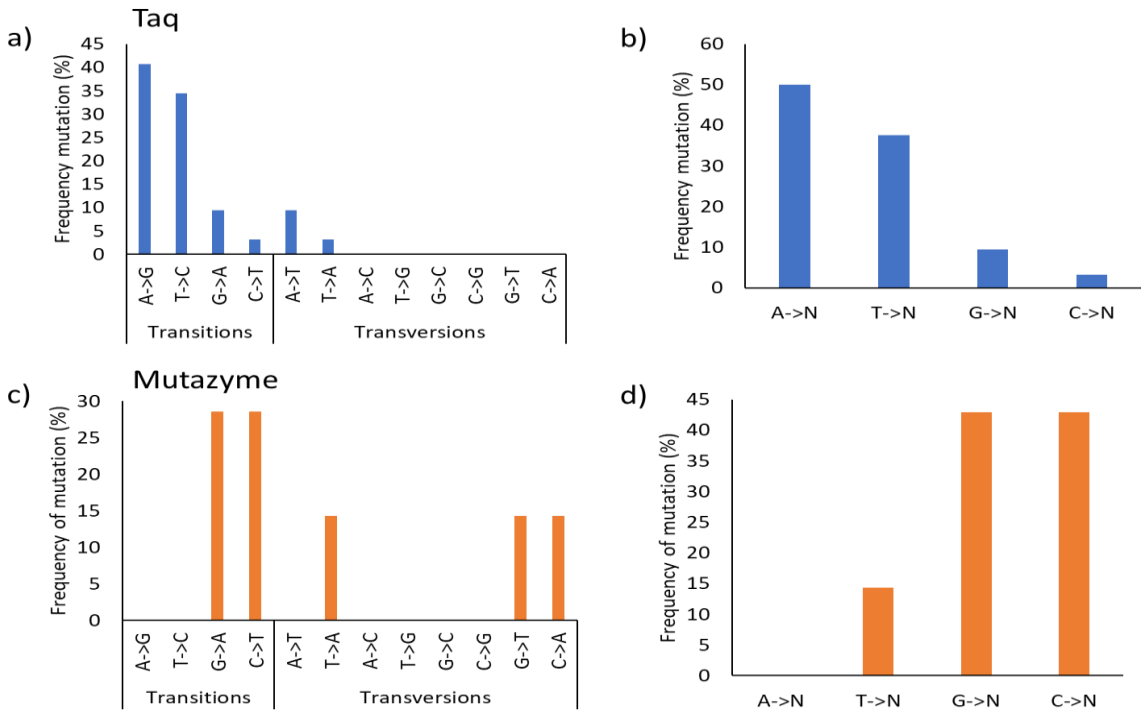

Figure 3.13: Mutational spectra of **a)** and **b)** Taq DNA polymerase and **c)** and **d)** Mutazyme II DNA polymerase in directed evolution studies with McoA.

It was also necessary to validate the McoA 15E6-loop5 variant, the parent of the next generation. The precision of the high-throughput methods used is of an utmost importance in assessing the evolvability characteristics of the parental enzyme of each generation and the mutant libraries quality. The implementation of efficient screening protocols, in which a reduced risk of selecting false positives is achieved, is therefore essential and requires an optimization of each of several steps throughout the process. In this study an activity-on-plate high-throughput screening and a liquid high-throughput screening, using 2,6-DMP as substrate, were performed as described in 2.15 and 2.18 (see Materials and Methods), respectively.

The activity-on-plate screening, in spite of its qualitative nature, allows for the screening of a higher number of clones in a shorter period of time as compared to a standardized 96-well plate assay. In Figure 3.14 it is possible to observe that all colonies showed an uniform orange color that represents the color of the product of the oxidation of 2,6-DMP. The optimization of the liquid high-throughput screening was also performed and a coefficient of variance (CV = standard deviation/mean × 100%) of ≈ 29% was achieved for maximal activity (1.5 ± 0.4 µmol/min·mL) in 4 different 96-well plates, ensuring the required reproducibility of the mcoA expression system to pursue the directed evolution studies (Figure 3.14b). Therefore the conditions to screen a library of variants and select best hits are validated and optimized.

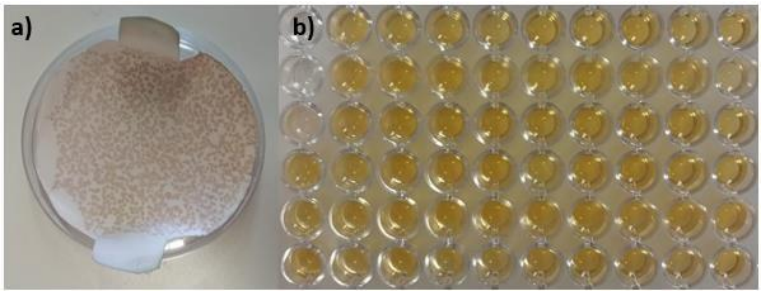

Figure 3.14: **a)** McoA 15E6-loop5 reaction with 2,6-DMP (1 mM) on a chromatography filter paper (“Activity-on-plate”) and **b)** McoA 15E6-loop5 reaction with 2,6-DMP (1 mM) on a 96-well plates (High- throughput screening).

4. Conclusions and Future Perspectives

Laccases are highly in demand enzymes for deconstruction and valorization of plant biomass for application in lignocellulosic biorefineries and other biotechnological applications due to their green catalytic properties, broad substrate specificity and the possibility of controlling reactivity by increasing or quenching O_2 partial pressure. Bacterial laccases although not as known and catalytic efficient compared to fungal laccases, possess higher optimal temperature, pH range, stability, salt tolerance and dispose of a greater number of genetic and molecular biology tools to improve their enzymatic properties for industrial applications (Brissos et al., 2015; Zhang et al., 2018).

Taking benefit of the bacterial systems well established genetic and molecular biological tools, Brissos et al. (2015) developed a lineage of laboratory evolved proteins from the metallo-oxidase McoA from *Aquifex aeolicus* for specificity improvement towards aromatic compounds that led to the 2B3 variant which showed better catalytic efficiency against ABTS than the native McoA. This variant was further evolved (results not published) for improved specificity towards the lignin-related phenolic compound, 2,6-DMP.

In the present study, the most recent descendants of this lineage of laboratory evolved proteins, the variants 15E6-loop5 and 23B3, were biochemically characterized and their activities towards a set of lignin-related phenolic compounds were assessed for the first time. The engineered laccases showed a slight alkali-tolerance increase compared to CotA for ABTS and for the majority of the phenolic compounds tested, which can be interpreted as an advantage for industrial processes carried out in alkaline conditions. Moreover, CotA-laccase oxidized all the thirteen tested phenolics substrates in contrast to the engineered laccases that have shown no enzymatic activity for syringaldehyde, acetosyringone, methylsyringate, vanillin and *p*-coumaric acid. However, for those oxidized by the native and both engineered laccases, McoA 15E6-loop5 showed more proximal catalytic efficiencies to those of CotA than 23B3, especially for sinapyl alcohol, 2,6-DMP, coniferyl alcohol and caffeic acid. In fact, the lower catalytic efficiencies observed for the engineered laccase towards some phenolics when compared to CotA, always at the same order of magnitude, are mostly due to the higher K_m values since the k_{cat} values are very similar.

Furthermore, to the best of our knowledge, this study was the first to optimize conditions for the dimerization of sinapyl alcohol using bacterial laccases. At first a reaction using CotA under the enzyme's optimal pH and at a temperature of 37°C, using ethanol as co-solvent and with immediate enzyme addition, resulted in a mixture of oligomers. However, by upshifting the temperature to 50°C, increasing the substrate:enzyme concentration ratio, adding the enzyme solution in slow mode and changing the co-solvent to acetonitrile as well as the pH medium to 10 in order to deprotonate the substrate, the dimeric form of sinapyl alcohol, syringaresinol, was obtained as major product of reaction. Under the same conditions, McoA 15E6-loop5 oxidative reaction also yielded syringaresinol, however not as the only product. The obtained results also showed that the formation of syringaresinol was, apart from the increased temperature and the co-solvent, promoted by the pH conditions where the enzymatic activity is lower and the sinapyl alcohol's protonation state, since while deprotonated (at pH 9.4 or higher), the monolignol is more prone to be oxidized. It is important to highlight that syringaresinol is

known for its medical properties like attenuation of inflammatory responses (Bajpai et al., 2018) and inhibition of *Helicobacter pylori* motility which is responsible for gastric cancer (Jaufurally et al., 2016). Plus, due to its two phenols and its rigid cis-fused bis-furanic moiety, is considered a potential substitute of the good-mechanically however endocrine disruptor bisphenol A for composition of polycarbonate plastics and epoxy resins (Jaufurally et al., 2016). The chemical processes for obtaining syringaresinol requires several solvent extractions and column chromatography purifications yielding small amounts of syringaresinol.

In conclusion, 15E6-loop5 variant performance is still lower than that of a laccase and a few more rounds of directed evolution would allow to improve their properties. This would results in an increased number of useful enzymes for lignocellulose biorefinery and for industrial processes for the synthesis of interesting products. As previously mentioned, these engineering approaches will allow also a better comprehension of the structure-function relationships in the family of the multicopper-oxidases. We have attempted to optimize conditions to further evolve the 15E6-loop5 variant. Until now, the evolution lineage was performed using the Taq DNA polymerase which is a biased enzyme for epPCR. We showed that the use of the less unbiased polymerase such as Mutazyme II is a promising alternative to Taq polymerase and although we were not able to accomplish this work and identify an improved variant, we believe that the studies performed paved the way to the set-up of successful evolution of 15E6-loop5 McoA variant.

References

Abdel-Hamid, A. M., Solbiati, J. O., & Cann, I. K. (2013). Insights into lignin degradation and its potential industrial applications. *Advances in applied microbiology*, *82*, 1–28. doi:10.1016/B978-0-12-407679-2.00001-6

Abdelaziz, O. Y., Brink, D. P., Prothmann, J., Ravi, K., Sun, M., García-Hidalgo, J., Sandahl, M., Hulteberg, C. P., Turner, C., Lidén, G., & Gorwa-Grauslund, M. F. (2016). Biological valorization of low molecular weight lignin. *Biotechnology advances*, *34*(8), 1318–1346. doi:10.1016/j.biotechadv.2016.10.001

Arregui, L., Ayala, M., Gómez-Gil, X., Gutiérrez-Soto, G., Hernández-Luna, C. E., Herrera de Los Santos, M., Levin, L., Rojo-Domínguez, A., Romero-Martínez, D., Saparrat, M., Trujillo-Roldán, M. A., & Valdez-Cruz, N. A. (2019). Laccases: structure, function, and potential application in water bioremediation. *Microbial cell factories*, *18*(1), 200. doi:10.1186/s12934-019-1248-0

Ázar, R., Bordignon-Junior, S. E., Laufer, C., Specht, J., Ferrier, D., & Kim, D. (2020). Effect of lignin content on cellulolytic saccharification of liquid hot water pretreated sugarcane bagasse. *Molecules (Basel, Switzerland)*, *25*(3), 623. doi:10.3390/molecules25030623

Bajpai, V. K., Alam, M. B., Quan, K. T., Ju, M. K., Majumder, R., Shukla, S., Huh, Y. S., Na, M., Lee, S. H., & Han, Y. K. (2018). Attenuation of inflammatory responses by (+)-syringaresinol via MAP-Kinase-mediated suppression of NF-κB signaling in vitro and in vivo. *Scientific reports*, *8*(1), 9216. doi:10.1038/s41598-018-27585-w

Barros, J., Serk, H., Granlund, I., & Pesquet, E. (2015). The cell biology of lignification in higher plants. *Annals of botany*, *115*(7), 1053–1074. doi:10.1093/aob/mcv046

Benvidi, A., Dadras, A., Abbasi, S., Tezerjani, M. D., Rezaeinasab, M., Tabaraki, R., & Namazian, M. (2019). Experimental and computational study of the pK_a of coumaric acid derivatives. *Journal of the Chinese Chemical Society*, *66*(6), 589-593. doi:10.1002/jccs.201800265

Bilal, M., & Iqbal, H. M. N. (2020). Ligninolytic enzymes mediated ligninolysis: An untapped biocatalytic potential to deconstruct lignocellulosic molecules in a sustainable manner. *Catalysis letters*, *150*, 524-543. doi:10.1007/s10562-019-03096-9

Bonechi, C., Consumi, M., Donati, A., Leone, G., Magnani, A., Tamasi, G., & Rossi, C. (2017). Biomass: An overview. In: Dalena, F., Basile, A., Rossi, C. (Eds.) *Bioenergy systems for the future: Prospects for biofuels and biohydrogen*. Kidlington, United Kingdom, Elsevier, pp. 3-42. doi:10.1016/b978-0-08-101031-0.00001-6

Bradford, M. M. (1976). A rapid and sensitive method for the quantitation of microgram quantities of protein utilizing the principle of protein-dye binding. *Analytical biochemistry*, *72(*1-2), 248– 254. doi:10.1016/0003-2697(76)90527-3

Brander, S., Mikkelsen, J. D., & Kepp, K. P. (2014). Characterization of an alkali- and halide-resistant laccase expressed in *E. coli*: CotA from *Bacillus clausii*. *Public library of Science one*, *9*(6), e99402. doi:10.1371/journal.pone.0099402

Brenner, A. J., & Harris, E. D. (1995). A quantitative test for copper using bicinchoninic acid. *Analytical biochemistry, 226*(1), 80–84. doi:10.1006/abio.1995.1194

Brigham, C. (2018). Biopolymers: Biodegradable alternatives to traditional plastics. In: Török, B., Dransfield, T. (Eds.). *Green chemistry: An inclusive approach*. Amsterdam, Netherlands, Elsevier, pp. 753-770. doi:10.1016/b978-0-12-809270-5.00027-3

Brissos, V., Chen, Z., & Martins, L. (2012). The kinetic role of carboxylate residues in the proximity of the trinuclear centre in the O2 reactivity of CotA-laccase. *Dalton transactions, 41*(20), 6247-6255.

doi:10.1039/c2dt12067d

Brissos, V., Ferreira, M., Grass, G., & Martins, L. O. (2015). Turning a hyperthermostable metallo-oxidase into a laccase by directed evolution. *American Chemical Society catalysis, 5*(8), 4932–4941. doi:10.1021/acscatal.5b00771

Borges, P., Brissos, V., Hernandez, G., Masgrau, L., Lucas, M. F., Monza, E., Frazão, C., Cordeiro, T., & Martins, L. O. (2020). The methionine-rich loop of multicopper oxidase McoA follows open-to-close transitions with a role in enzyme catalysis. *American Chemical Society catalysis*. doi:10.1021/acscatal.0c01623

Bugg, T. D., & Rahmanpour, R. (2015). Enzymatic conversion of lignin into renewable chemicals. *Current opinion in chemical biology*, *29*, 10-17. doi:10.1016/j.cbpa.2015.06.009

Bugg, T., Williamson, J. J., & Rashid, G. (2020). Bacterial enzymes for lignin depolymerisation: new biocatalysts for generation of renewable chemicals from biomass. *Current opinion in chemical biology*, *55*, 26–33. doi:10.1016/j.cbpa.2019.11.007

Calcaterra, A., Galli, C., & Gentili, P. (2008). Phenolic compounds as likely natural mediators of laccase: A mechanistic assessment. *Journal of molecular catalysis B: Enzymatic, 51*(3-4), 118– 120. doi:10.1016/j.molcatb.2007.11.023

Camarero, S., Ibarra, D., Martinez, M. J., & Martinez, A. T. (2005). Lignin-derived compounds as efficient laccase mediators for decolorization of different types of recalcitrant dyes. *Applied and environmental microbiology, 71*(4), 1775–1784. doi:10.1128/aem.71.4.1775

Camarero, S., Cañas, A. I., Nousiainen, P., Record, E., Lomascolo, A., Martínez, M. J., & Martínez, A. T. (2008). P-hydroxycinnamic acids as natural mediators for laccase oxidation of recalcitrant compounds. *Environmental science & technology*, *42*(17), 6703–6709. doi:10.1021/es8008979

Capolupo, L., & Faraco, V. (2016). Green methods of lignocellulose pretreatment for biorefinery development. *Applied microbiology and biotechnology*, *100*(22), 9451–9467. doi:10.1007/s00253-016-7884-y

Carunchio, F., Crescenzi, C., Girelli, A. M., Messina, A., & Tarola, A. M. (2001). Oxidation of ferulic acid by laccase: Identification of the products and inhibitory effects of some dipeptides. *Talanta*, *55*(1), 189–200. doi:10.1016/s0039-9140(01)00417-9

Chen, H. (2015). Lignocellulose biorefinery feedstock engineering. *Lignocellulose biorefinery engineering: Principles and applications*. Cambridge, United Kingdom, Elsevier, Woodhead Publishing, pp. 37-86. doi:10.1016/B978-0-08-100135-6.00003-X

Cherubini, F. (2010). The biorefinery concept: Using biomass instead of oil for producing energy and chemicals. *Energy conversion and management*, *51*(7), 1412-1421. doi:10.1016/j.enconman.2010.01.015

Clews, R.J. (2016). Chapter 5 – Fundamentals of the petroleum industry. *Project finance for the international petroleum industry.* London, United Kingdom, Elsevier, Academic Press, pp. 83-99. doi:10.1016/B978-0-12-800158-5.00005-0

D'Acunzo, F., & Galli, C. (2003). First evidence of catalytic mediation by phenolic compounds in the laccase-induced oxidation of lignin models. *European journal of biochemistry*, *270*(17), 3634–3640. doi:10.1046/j.1432-1033.2003.03752.x

Dávila, I., Gullón, B., Alonso, J., L., Labidi, J., & Gullón, P. (2019). Vine shoots as new source for the manufacture of prebiotic oligosaccharides. *Carbohydrate polymers*, *207*, 34-43. doi:10.1016/j.carbpol.2018.11.065

Delavari, A., & Perez, J.J. (2013). 210 Computational study of substrates and mediators features of lacasses, *Journal of biomolecular structure and dynamics*, *31*(sup1), 136-137. doi:10.1080/07391102.2013.790141

Durão, P., Chen, Z., Fernandes, A. T., Hildebrandt, P., Murgida, D. H., Todorovic, S., Pereira, M. M., Melo, E. P., & Martins, L. O. (2008). Copper incorporation into recombinant CotA laccase from Bacillus subtilis: characterization of fully copper loaded enzymes. *Journal of biological inorganic chemistry: A publication of the society of biological inorganic chemistry*, *13*(2), 183–193. doi:10.1007/s00775-007-0312-0

Durão, P., Chen, Z., Silva, C. S., Soares, C. M., Pereira, M. M., Todorovic, S., Hildebrandt, P., Bento, I., Lindley, P. F., & Martins, L. O. (2008). Proximal mutations at the type 1 copper site of CotA laccase: spectroscopic, redox, kinetic and structural characterization of I494A and L386A mutants. *The biochemical journal*, *412*(2), 339–346. doi:10.1042/BJ20080166

Fernandes, A. T., Soares, C. M., Pereira, M. M., Huber, R., Grass, G., & Martins, L. O. (2007). A robust metallo-oxidase from the hyperthermophilic bacterium *Aquifex aeolicus. The federation of European biochemical societies journal*, *274*(11), 2683–2694. doi:10.1111/j.1742-4658.2007.05803.x

Fernandes, A. T., Martins, L. O., & Melo, E. P. (2009). The hyperthermophilic nature of the metallo-oxidase from *Aquifex aeolicus. Biochimica et biophysica acta, 1794*(1), 75– 83. doi:10.1016/j.bbapap.2008.09.006

Fernandes, A. T., Damas, J. M., Todorovic, S., Huber, R., Baratto, M. C., Pogni, R., Soares, C. M., & Martins, L. O. (2010). The multicopper oxidase from the archaeon *Pyrobaculum aerophilum* shows nitrous oxide reductase activity. *The Federation of European Biochemical Societies journal*, *277*(15), 3176–3189. doi:10.1111/j.1742-4658.2010.07725.x

Foyle, T., Jennings, L., & Mulcahy, P. (2007). Compositional analysis of lignocellulosic materials: Evaluation of methods used for sugar analysis of waste paper and straw. *Bioresource technology, 98*(16), 3026–3036. doi:10.1016/j.biortech.2006.10.013

Fraser, C. M., & Chapple, C. (2011). The phenylpropanoid pathway in *Arabidopsis*. *The arabidopsis book*, *9*, e0152. doi:10.1199/tab.0152

Genaro-Mattos, T. C., Maurício, Â. Q., Rettori, D., Alonso, A., & Hermes-Lima, M. (2015). Antioxidant activity of caffeic acid against iron-induced free radical generation - A chemical approach. *Public library of Science one*, *10*(6), e0129963. doi:10.1371/journal.pone.0129963

Giardina, P., Faraco, V., Pezzella, C., Piscitelli, A., Vanhulle, S., & Sannia, G. (2010). Laccases: a never-ending story. *Cellular and molecular life sciences*, *67*(3), 369–385. doi:10.1007/s00018-009-0169-1

Gupta, A., Turner, S. R. (2017). Cellulose. In: Thomas, B., Murray, B. G., Murphy, D.J. (Eds.) *Encyclopedia of applied plant sciences. 2nd edition*. Oxford, Elsevier, Academic Press, pp. 185–90. doi:10.1016/B978-0-12-394807-6.00115-5.

Hatti-Kaul, R. & Ibrahim, V. (2013). Lignin-degrading enzymes: An overview. In: Yang, S. T., El-Enshasy, H., Tongchul, N. (Eds.) *Bioprocessing technologies in biorefinery for sustainable production of fuels, chemicals, and polymer*s. New York, United States, Wiley, pp. 67–192. doi:10.1002/9781118642047.ch10

Henriques, A. O., & Moran, C. P., Jr (2000). Structure and assembly of the bacterial endospore coat. *Methods*, *20*(1), 95–110. doi:10.1006/meth.1999.0909

Higuchi, T. (1997). Structure and functions of wood. In: *Biochemistry and molecular biology of wood*. Berlin, Heidelberg, Springer-Verlag, pp. 1– 40. doi: 10.1007/978-3-642-60469-0

Höfte, H., Gonneau, M., & Vernhettes, S. (2007). 2.22 - Biosynthesis of cellulose. In: Kamerling, J. P.

(Ed.). *Comprehensive glycoscience: From chemistry to systems biology, 2.* Oxford, United Kingdom, Elsevier, pp. 737–763. doi:10.1016/b978-044451967-2/00142-2

Jähnert, T., Hager, M. D., & Schubert, U. S. (2014). Application of phenolic radicals for antioxidants, as active materials in batteries, magnetic materials and ligands for metal-complexes. *Journal of materials chemistry A, 2*(37), 15234-15251. doi:10.1039/c4ta03023k

Janusz, G., Pawlik, A., Sulej, J., Świderska-Burek, U., Jarosz-Wilkołazka, A., & Paszczyński, A. (2017). Lignin degradation: microorganisms, enzymes involved, genomes analysis and evolution. *Federation of European microbiological societies microbiology reviews, 41*(6), 941–962. doi:10.1093/femsre/fux049

Jaufurally, A. S., Teixeira, A. R. S., Hollande, L., Allais, F., & Ducrot, P.-H. (2016). Optimization of the laccase-catalyzed synthesis of (±)-syringaresinol and study of its thermal and antiradical activities. *ChemistrySelect, 1*(16), 5165–5171. doi: 10.1002/slct.201600543

Jędrzejczyk, M., Soszka, E., Czapnik, M., Ruppert, A. M., & Grams, J. (2019). Chapter 6 - Physical and chemical pretreatment of lignocellulosic biomass. In: Basile, A., Dalena, F. (Eds.). *Second and third generation of feedstocks: The evolution of biofuels.* Elsevier, pp. 143–196. doi:10.1016/b978-0-12-815162-4.00006-9

Jones, S. M., & Solomon, E. I. (2015). Electron transfer and reaction mechanism of laccases. *Cellular and molecular life sciences, 72*(5), 869–883. doi:10.1007/s00018-014-1826-6

Kajiyama, T., & Ohkatsu, Y. (2001). Effect of para-substituents of phenolic antioxidants. *Polymer degradation and stability, 71*(3), 445–452. doi:10.1016/s0141-3910(00)00196-8

Kamm, B., & Kamm, M. (2004). Principles of biorefineries. *Applied microbiology and biotechnology, 64*(2), 137–145. doi:10.1007/s00253-003-1537-7

Kamm, B., Schneider, B., Hüttl, R.F., Grünewald, H., Gusovius, H., Stollberg, C., Ay, P., & Kamm, M. (2006). Lignocellulosic feedstock biorefinery - Combination of technologies of agroforestry and a biobased substance and energy economy. *Forum der forschung, 19*, 53-62. Available from: https://www.researchgate.net/publication/242538853

Kawai, S., Asukai, M., Ohya, N., Okita, K., Ito, T., & Ohashi, H. (1999). Degradation of a non-phenolic β-O-4 substructure and of polymeric lignin model compounds by laccase of *Coriolus versicolor* in the presence of 1-hydroxybenzotriazole. *Federation of European microbiological societies microbiology letters, 170*(1), 51–57. doi:10.1111/j.1574-6968.1999.tb13354.x

Kishimoto, T., Takahashi, N., Hamada, M., & Nakajima, N. (2015). Biomimetic oxidative coupling of sinapyl acetate by silver oxide: Preferential formation of β-O-4 type structures. *Journal of agricultural and food chemistry, 63*(8), 2277–2283. doi:10.1021/jf506111q

Klemm, D., Heublein, B., Fink, H. P., & Bohn, A. (2005). Cellulose: Fascinating biopolymer and sustainable raw material. *Angewandte chemie international edition, 44*(22), 3358– 3393. doi:10.1002/anie.200460587

Knaggs A. R. (2003). The biosynthesis of shikimate metabolites. *Natural product reports*, *20*(1), 119–136. doi:10.1039/b100399m

Konwar, L. J., Mikkola, J.-P., Bordoloi, N., Saikia, R., Chutia, R. S., & Kataki, R. (2018). Chapter 3 - Sidestreams from bioenergy and biorefinery complexes as a resource for circular bioeconomy. In: Bhaskar, T., Pandey, A., Mohan, S. V., Lee, D, & Khanal, S. (Eds.). *Waste biorefinery: Potential and perspectives.* Amsterdam, Netherlands, Elsevier, pp. 85–125. doi:10.1016/b978-0-444-63992-9.00003-3

Koschorreck, K., Richter, S. M., Ene, A. B., Roduner, E., Schmid, R. D., & Urlacher, V. B. (2008). Cloning

and characterization of a new laccase from *Bacillus licheniformis* catalyzing dimerization of phenolic acids. *Applied microbiology and biotechnology*, *79*(2), 217–224. doi:10.1007/s00253-008-1417-2

Kosman D. J. (2002). FET3P, ceruloplasmin, and the role of copper in iron metabolism. *Advances in protein chemistry*, *60*, 221–269. doi:10.1016/s0065-3233(02)60055-5

Kumar, A., & Chandra, R. (2020). Ligninolytic enzymes and its mechanisms for degradation of lignocellulosic waste in environment. *Heliyon, 6*(2), e03170. doi:10.1016/j.heliyon.2020.e03170

Kumar, P., Barrett, D. M., Delwiche, M. J., & Stroeve, P. (2009). Methods for pretreatment of lignocellulosic biomass for efficient hydrolysis and biofuel production. *Industrial & engineering chemistry research, 48*(8), 3713–*3729.* doi:10.1021/ie801542g

Kwan, D. H. (2017). Chapter Two - Structure-guided directed evolution of glycosidases: A case study in engineering a blood group antigen-cleaving enzyme. In: Imperiali, B. (Ed.). *Methods in enzymology*, *597*, pp. 25–53. doi:10.1016/bs.mie.2017.06.002

Laurichesse, S., & Avérous, L. (2014). *Chemical modification of lignins: Towards biobased polymers. Progress in polymer science, 39*(7), 1266–1290. doi:10.1016/j.progpolymsci.2013.11.004

Lourenço, A., & Pereira, H. (2018). Compositional variability of lignin in biomass. In: Poletto, M. (Ed.). *Lignin: trends and applications.* IntechOpen, pp. 65-98 doi:10.5772/intechopen.71208

Madzak, C., Mimmi, M. C., Caminade, E., Brault, A., Baumberger, S., Briozzo, P., Mougin, C., & Jolivalt, C. (2006). Shifting the optimal pH of activity for a laccase from the fungus *Trametes versicolor* by structure-based mutagenesis. *Protein engineering, design & selection, 19*(2), 77–84. doi:10.1093/protein/gzj004

Martins, L. O., Soares, C. M., Pereira, M. M., Teixeira, M., Costa, T., Jones, G. H., & Henriques, A. O. (2002). Molecular and biochemical characterization of a highly stable bacterial laccase that occurs as a structural component of the *Bacillus subtilis* endospore coat. *The Journal of biological chemistry*, *277*(21), 18849–18859. doi:10.1074/jbc.M200827200

Martins, L. O., Durão, P., Brissos, V., & Lindley, P. F. (2015). Laccases of prokaryotic origin: enzymes at the interface of protein science and protein technology. *Cellular and molecular life sciences, 72*(5), 911–922. doi:10.1007/s00018-014-1822-x

McKendry, P. (2002). Energy production from biomass (part 1): Overview of biomass. *Bioresource technology, 83*(1), 37–46. doi:10.1016/s0960-8524(01)00118-3

Mehra, R., Muschiol, J., Meyer, A. S., & Kepp, K. P. (2018). A structural-chemical explanation of fungal laccase activity. *Scientific reports, 8*(1). doi:10.1038/s41598-018-35633-8

Monlau, F., Barakat, A., Trably, E., Dumas, C., Steyer, J.-P., & Carrère, H. (2013). Lignocellulosic materials into biohydrogen and biomethane: Impact of structural features and pretreatment. *Critical reviews in environmental science and technology, 43*(3), 260–
322. doi:10.1080/10643389.2011.604258

Morsi, R., Bilal, M., Iqbal, H. M. N., & Ashraf, S. S. (2020). Laccases and peroxidases: The smart, greener and futuristic biocatalytic tools to mitigate recalcitrant emerging pollutants. *Science of the total environment, 714,* 136572. doi:10.1016/j.scitotenv.2020.136572

Nemadziva, B., Le Roes-Hill, M., Koorbanally, N., & Kudanga, T. (2018). Small laccase-catalyzed synthesis of a caffeic acid dimer with high antioxidant capacity. *Process biochemistry, 69,* 99– 105. doi:10.1016/j.procbio.2018.03.009

NET - https://foodb.ca/compounds/FDB031178

Ozawa, M., Fukutome, A., Sannami, Y., Kamitakahara, H., & Takano, T. (2014). Preparation and evaluation of the oxidation ability of hematin-appended 6-amino-6-deoxycellulose. *Journal of the wood chemistry and technology, 34*(4), 262-272. doi:10.1080/02773813.2013.869605

Pande M., & Bhaskarwar, A. N. (2012). Biomass conversion to energy. In: Baskar, C., Baskar, S., Dhillon, R. S. (Eds.) *Biomass conversion*: *The interface of biotechnology, chemistry and materials science*. Berlin, Heidelberg, Springer pp. 2-90. doi:10.1007/978-3-642-28418-2_1

Pardo, I., & Camarero, S. (2015). Exploring the oxidation of lignin-derived phenols by a library of laccase mutants. *Molecules (Basel, Switzerland)*, *20*(9), 15929–15943. doi:10.3390/molecules200915929

Pérez, J., Muñoz-Dorado, J., de la Rubia, T., & Martínez, J. (2002). Biodegradation and biological treatments of cellulose, hemicellulose and lignin: an overview. *International microbiology : the official journal of the Spanish Society for Microbiology*, *5*(2), 53–63. doi:10.1007/s10123-002-0062-3

Ragauskas, A. J., Beckham, G. T., Biddy, M. J., Chandra, R., Chen, F., Davis, M. F., Davison, B. H., Dixon, R. A., Gilna, P., Keller, M., Langan, P., Naskar, A. K., Saddler, J. N., Tschaplinski, T. J., Tuskan, G. A., & Wyman, C. E. (2014). Lignin valorization: improving lignin processing in the biorefinery. *Science, 344*(6185), 1246843. doi:10.1126/science.1246843

Ragauskas, A. J., & Yoo, C. G. (2018). Editorial: Advancements in biomass recalcitrance: The use of lignin for the production of fuels and chemicals. *Frontiers in energy research, 6.* doi:10.3389/fenrg.2018.00118

Ragnar, M., Lindgren, C. T., & Nilvebrant, N.-O. (2000). pKa-values of guaiacyl and syringyl phenols related to lignin. *Journal of wood chemistry and technology, 20*(3), 277– 305. doi:10.1080/02773810009349637

Reano, A. F., Pion, F., Domenek, S., Ducrot, P.-H., & Allais, F. (2016). Chemo-enzymatic preparation and characterization of renewable oligomers with bisguaiacol moieties: Promissing sustainable antiradical/antioxidant additives. *Green chemistry, 18*(11), 3334-3345. doi: 10.1039/C6GC00117C

Reiss, R., Ihssen, J., & Thöny-Meyer, L. (2011). *Bacillus pumilus* laccase: a heat stable enzyme with a wide substrate spectrum. *BioMed Central biotechnology, 11*(1), 9. doi:10.1186/1472-6750-11-9

Reiss, R., Ihssen, J., Richter, M., Eichhorn, E., Schilling, B., & Thöny-Meyer, L. (2013). Laccase versus laccase-like multi-copper oxidase: a comparative study of similar enzymes with diverse substrate spectra. *Public library of Science one*, *8*(6), e65633. doi:10.1371/journal.pone.0065633

Rosado, T., Bernardo, P., Koci, K., Coelho, A. V., Robalo, M. P., & Martins, L. O. (2012). Methyl syringate: An efficient phenolic mediator for bacterial and fungal laccases. *Bioresource technology, 124,* 371–378. doi:10.1016/j.biortech.2012.08.023

Ruiz-Dueñas, F. J., & Martínez, A. T. (2009). Microbial degradation of lignin: how a bulky recalcitrant polymer is efficiently recycled in nature and how we can take advantage of this. *Microbial biotechnology*, *2*(2), 164–177. doi:10.1111/j.1751-7915.2008.00078.x

Scheller, H. V., & Ulvskov, P. (2010). Hemicelluloses. *Annual review of plant biology*, *61*, 263–289. doi:10.1146/annurev-arplant-042809-11231

Shu, R., Li, R., Lin, B., Wang, C., Cheng, Z., & Chen, Y. (2020). A review on the catalytic hydrodeoxygenation of lignin-derived phenolic compounds and the conversion of raw lignin to hydrocarbon liquid fuels. *Biomass and bioenergy, 132*, 105432. doi: 10.1016/j.biombioe.2019.105432

Silva, C. S., Durão, P., Fillat, A., Lindley, P. F., Martins, L. O., & Bento, I. (2012). Crystal structure of the multicopper oxidase from the pathogenic bacterium *Campylobacter jejuni*CGUG11284: Characterization of a metallo-oxidase. *Metallomics: integrated biometal science, 4*(1), 37–47. doi: doi.org/10.1039/c1mt00156f

Singh, S. K., Grass, G., Rensing, C., & Montfort, W. R. (2004). Cuprous oxidase activity of CueO from *Escherichia coli*. *Journal of bacteriology*, *186*(22), 7815–7817. doi:10.1128/JB.186.22.7815-7817.2004

Sjöstrom, E. (1993). *Wood chemistry: Fundamentals and applications, 2*. New York, United States, Elsevier, Academic Press. doi:10.1016/C2009-0-03289-9

Smirnov, S. A., Koroleva, O. V., Gavrilova, V. P., Belova, A. B., & Klyachko, N. L. (2001). *Biochemistry (Moscow), 66*(7), 774–779. doi:10.1023/a:1010216829856

Springob, K., & Kutchan, T. M. (2009). Introduction to the different classes of natural products. In: Osbourn, A. E., Lanzotti, V. (Eds.). *Plant-derived natural products: Synthesis, function, and application,* Springer, pp. 3–50. doi:10.1007/978-0-387-85498-4_1

Strassberger, Z., Tanase, S., & Rothenberg, G. (2014). The pros and cons of lignin valorisation in an integrated biorefinery. *Royal Society of Chemistry advances, 4(48),* 25310– 25318. doi:10.1039/c4ra04747h

Sturgeon, M. R., Kim, S., Lawrence, K., Paton, R. S., Chmely, S. C., Nimlos, M., Foust, T. D., & Beckham, G. T. (2013). A mechanistic investigation of acid-catalyzed cleavage of aryl-ether linkages: Implications for lignin depolymerization in acidic environments. *American Chemical Society sustainable chemistry & engineering, 2*(3), 472–485. doi:10.1021/sc400384w

Sun, Z., Fridrich, B., de Santi, A., Elangovan, S., & Barta, K. (2018). Bright side of lignin depolymerization: Toward new platform chemicals. *Chemical reviews*, *118*(2), 614–678. doi:10.1021/acs.chemrev.7b00588

Tobimatsu, Y., & Schuetz, M. (2019). Lignin polymerization: How do plants manage the chemistry so well? *Current opinion in biotechnology, 56*, 75-81. doi: 10.1016/j.copbio.2018.10.001

Tolbert, A., Akinosho, H., Khunsupat, R., Naskar, A. K., & Ragauskas, A. J. (2014). Characterization and analysis of the molecular weight of lignin for biorefining studies. *Biofuels, bioproducts and biorefining, 8*(6), 836–856. doi: 10.1002/bbb.1500

Ummalyma, S. B., Supriya, R. D., Sindhu, R., Binod, P., Nair, R. B., Pandey, A., & Gnansounou, E. (2019). Chapter 7 - Biological pretreatment of lignocellulosic biomass - Current trends and future perspectives. In: Basile, A., Dalena, F. (Eds.). *Second and third generation of feedstocks: The evolution of biofuels.* Elsevier, pp. 197–212. doi:10.1016/b978-0-12-815162-4.00007-0

Vanholme, R., Demedts, B., Morreel, K., Ralph, J., & Boerjan, W. (2010). Lignin biosynthesis and structure. *Plant physiology, 153*(3), 895–905. doi:10.1104/pp.110.155119

Vassão, D. G., Davin, L. B., & Lewis, N. G. (2008). Chapter 13 - Metabolic engineering of plant allyl/propenyl phenol and lignin pathways: Future potential for biofuels/bioenergy, polymer intermediates, and specialty chemicals? In: Bonhert, H. J., Nguyen, H., Lewis, N. G. (Eds.). *Advances in plant biochemistry and molecular biology: Bioengineering and molecular biology of plant pathways, 1,* Elsevier, pp. 385–428. doi:10.1016/s1755-0408(07)01013-2

Wan, Y., Lu, R., Akiyama, K., Miyakoshi, T., & Du, Y. (2007). Enzymatic synthesis of bioactive compounds by *Rhus* laccase from Chinese *Rhus vernicifera*. *Science in China series B: Chemistry, 50*(2), 179–182. doi:10.1007/s11426-007-0022-z

Xie, T., Liu, Z., Liu, Q., & Wang, G. (2015). Structural insight into the oxidation of sinapic acid by CotA laccase. *Journal of structural biology, 190*(2), 155–161. doi:10.1016/j.jsb.2015.03.005

Yousuf, A. (2012). Biodiesel from lignocellulosic biomass – Prospects and challenges. *Waste management, 32*(11), 2061–2067. doi:10.1016/j.wasman.2012.03.008

Zakzeski, J., Bruijnincx, P. C., Jongerius, A. L., & Weckhuysen, B. M. (2010). The catalytic valorization of lignin for the production of renewable chemicals. *Chemical reviews*, *110*(6), 3552–3599. doi:10.1021/cr900354u

Zhang, G., Chen, Y., & Du, G. (2020). Chapter 7 – Protein engineering approaches for enhanced catalytic efficiency. In: Singh, S. P., Pandey, A., Singhania, R. R., Larroche, C., Li, Z. (Eds.). *Biomass, biofuels, biochemicals: Advances in enzyme catalysis and technologies,* Amsterdam, Netherlands, Elsevier, pp. 103-117. doi:10.1016/B978-0-12-819820-9.00007-7

Zhang, J., Ma, F., Zhang, X., & Geng, A. (2018). Directed Evolution of a Homodimeric Laccase from *Cerrena unicolor* BBP6 by Random Mutagenesis and In Vivo Assembly. *International journal of molecular sciences*, *19*(10), 2989. doi:org/10.3390/ijms19102989

Zheng, Y., Shi, J., Tu, M., & Cheng, Y.-S. (2017). Chapter One - Principles and development of lignocellulosic biomass pretreatment for biofuels. In: *Advances in bioenergy, 2,* Elsevier, Academic Press, pp. 1-68. doi:10.1016/bs.aibe.2017.03.001

Appendice section

Annex A - Protein quantification by Bradford method

In order to measure the protein concentration using the Bradford assay, the standard curve of absorbance at 595 nm versus bovine serum albumin (BSA) with known concentrations was constructed and shown in figure S1.

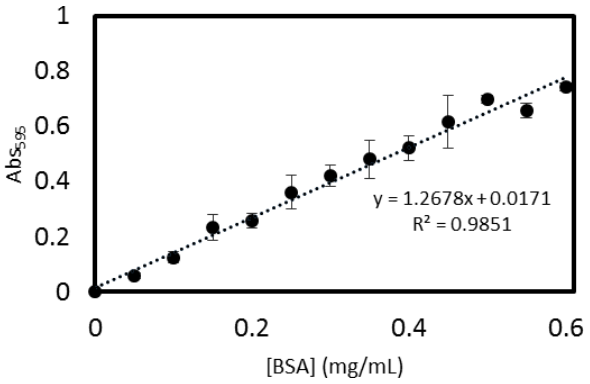

Figure S1: Standard curve for protein quantification

Annex B - Copper quantification

To determine the copper concentration in the protein, mentioned in 2.8 (see Materials and Methods), the standard curve was constructed and is represented in figure S2 with equation y = 0.0087 x + 0.0351. The absorbance values at 354.5 nm for the proteins were applied in the calibration curve and the copper content determined.

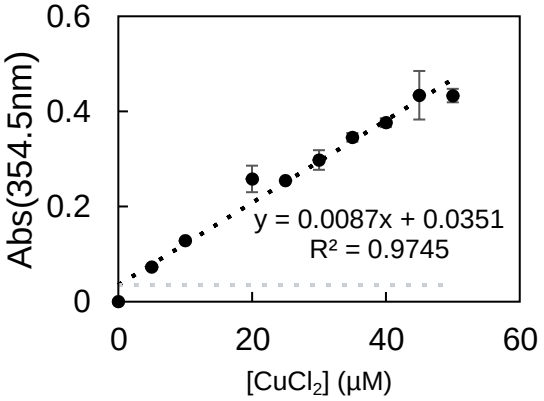

Figure S2: Standard curve for quantification of copper in enzyme preparations.

Annex C – Lignin-related phenolic compounds molar extinction coefficient determination

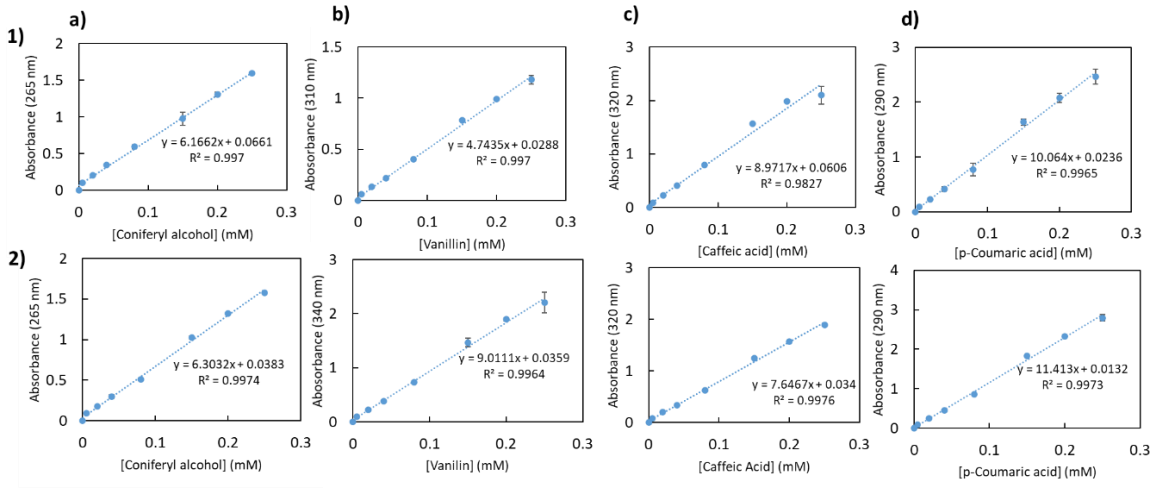

Figure S3: Standard curves of absorbance versus concentration for a) coniferyl alcohol (mM); b) vanillin (mM);
c) caffeic acid and d) *p*-coumaric acid to determine coefficient of exctinction at 1) pH 4 and 2) pH 8.

Annex D – Michaelis-Menten kinetics

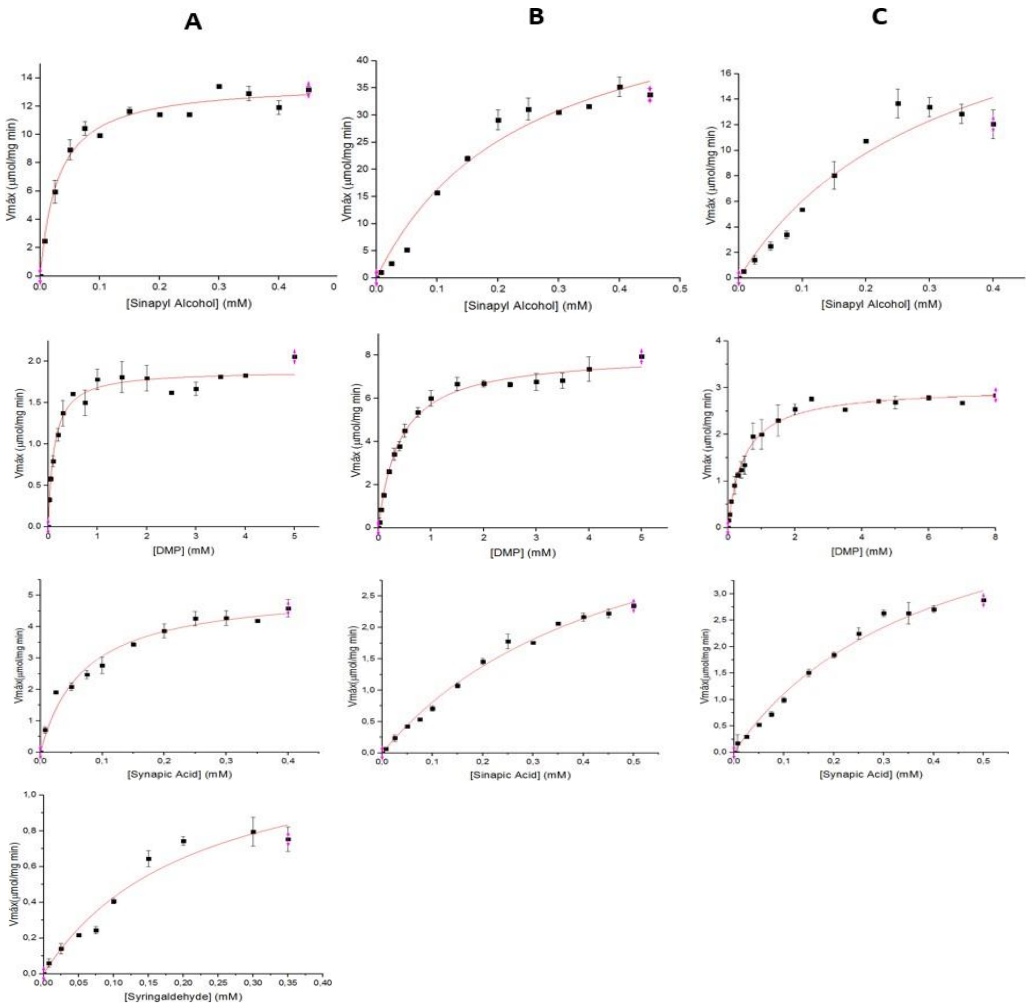

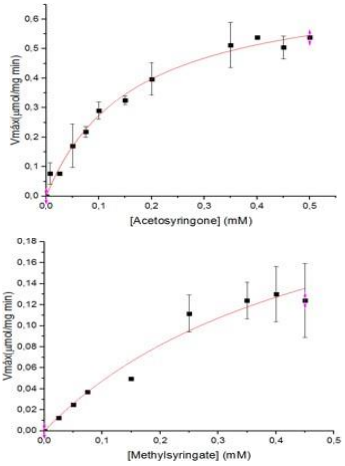

Figure S4: Michaelis-Menten kinetics of **(A)** CotA, **(B)** McoA 15E6-loop5 and **(C)** McoA 23B3 towards syringyl-type phenolic substrates (non-linear regression using Origin-Lab software).

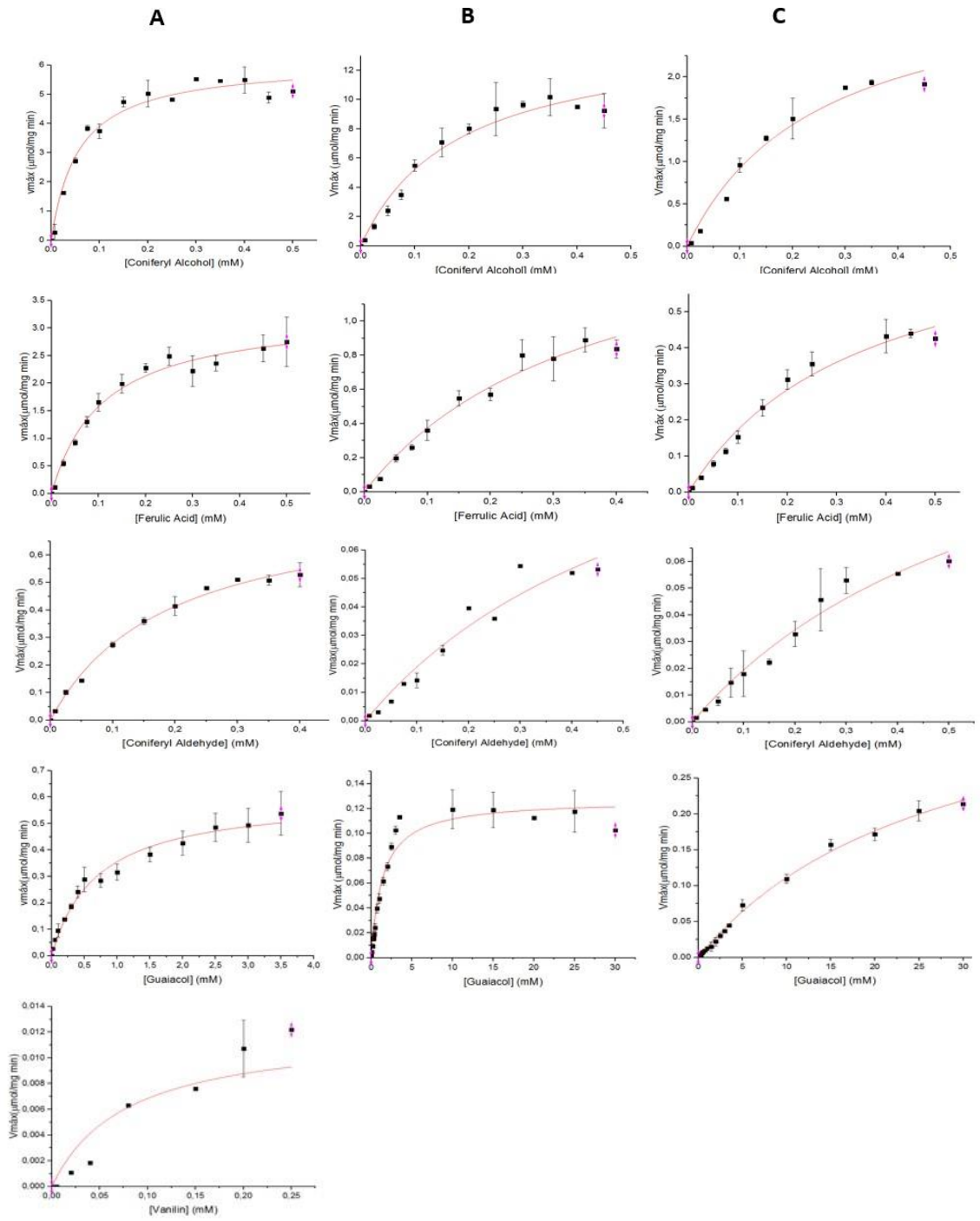

Figure S5: Michaelis-Menten kinetics using **(A)** CotA, **(B)** McoA 15E6-loop5 and **(C)** McoA 23B3 towards guaiacyl-type phenolic substrates (non-linear regression using Origin-Lab software).